

This is the final version of a submitted manuscript accepted for publication by the Journal Hydrological Processes on the 21st September 2022. The published article DOI is: 10.1002/hyp.14709

Application of Environmental Magnetism to Estimate Source Contribution by Lithology to Kruger National Park Reservoirs

Miller, J.K.¹, Rowntree, K.M.¹, Foster, I.D.L.^{1,2}, Reinwarth, B.³ and Baade, J.³

¹ Department of Geography, Rhodes University, South Africa

² Environmental and Geographical Sciences, Northampton University; United Kingdom

³ Department of Geography, Friedrich-Schiller-University Jena, Germany

Corresponding Author: Jordan Miller, jordy.k.miller@gmail.com

Abstract

Sediment source fingerprinting using environmental magnetism has successfully differentiated between sediment sources in several studies in the Eastern Cape Province of South Africa. The method was applied in this study to the near-natural landscape of southern Kruger National Park (Mpumalanga Province) to trace sediment and determine sediment yields by lithology in four reservoir catchments that were underlain by igneous, metamorphic, and sedimentary rocks. The Park area has no history of cultivation and is a conservation area, so catchment sources were dominated by underlying lithologies. One sediment core was collected in the assumed deepest area of the reservoir. Source discrimination and apportionment were estimated using a common statistical protocol that includes a Mann-Whitney U or Kruskal-Wallis H test, mass conservation test, discriminant function analysis, and an (un)mixing model. A contribution from each lithology-defined source was estimated. Sediment yield by lithology was estimated by using published catchment area-specific sediment yields in combination with the (un)mixing model. Underlying lithology determined vegetation type and density, and vegetation appeared to play a crucial role in protecting soils and reducing erosion. Proximity to reservoir, i.e., travel distance for eroded sediment, and connectivity were also important factors controlling the relative contribution from each potential source. The contributing area for sediment was found to be dynamic through time and was probably dependent on runoff and temporal variations in vegetation cover.

Keywords: environmental magnetism, sediment source fingerprinting, sediment tracing, erosion, connectivity, Kruger National Park.

1. INTRODUCTION

Southern Africa has a poor database of sediment yields and what data there are come largely from river monitoring and reservoir surveys conducted before the start of the current millennium (Vanmaercke *et al.*, 2014). Available data suggest sediment yields are some of the highest on the African continent (Walling and Webb 1996, Vanmaercke *et al.* 2014, Foster and Boardman, 2018). Most studies have focused on sediment yields from erosion-prone catchments and areas dominated by agricultural land (especially grazing) and high population densities, and few have focused on areas of the continent unaffected by human impacts. Overgrazing has often led to land degradation and yields exceeding $1000 \text{ t km}^{-2} \text{ yr}^{-1}$. It is estimated that 70 % of South Africa is affected by water erosion, and the most destructive forms of soil degradation are sheet and gully erosion (Garland *et al.*, 2000; Le Roux *et al.*, 2008) as well as soil crusting and compaction (Snyman and Du Preez, 2005). Manjoro (2011) implies that semi-arid areas are particularly prone to, and impacted by, soil erosion. There is minimal available information on soil erosion in natural veld landscapes (Snyman and Van Rensburg, 1986; Garland, 1995; Garland *et al.*, 2000). Average soil loss on erosion plots in near-natural veld in the Gauteng province between the 1930s and 1950s was $25 - 50 \text{ t km}^{-2} \text{ yr}^{-1}$ (Haylett, 1960). Venter (1988) estimated soil loss from experimental plots of $25 \text{ t km}^{-2} \text{ yr}^{-1}$ in a South African game reserve with a normal game population, but this increased to $75 \text{ t km}^{-2} \text{ yr}^{-1}$ for a high game population. Hoffman and Ashwell (2001) reviewed South African literature on undisturbed veld and estimated soil loss of $2 - 75 \text{ t km}^{-2} \text{ yr}^{-1}$. Kruger National Park (KNP) offered a further opportunity to trace sediment sources and reconstruct sediment yields in a largely human-free landscape dominated by indigenous fauna and no history of European farming activities. Baade *et al.* (2012) calculated mean area-specific sediment yield values of $10 - 60 \text{ t km}^{-2} \text{ yr}^{-1}$ in southern Kruger National Park (KNP) reservoirs. In a follow up study, Reinwarth *et al.* (2019) reported sediment yields for 15 reservoir catchments of between 5 ± 1 to $80 \pm 20 \text{ t km}^{-2} \text{ yr}^{-1}$ with a mean of $30 \pm 10 \text{ t km}^{-2} \text{ yr}^{-1}$. Catchments are not homogenous with respect to erosion rates and sediment delivery. The study reported here used four of the same reservoir catchments from Reinwarth *et al.*'s (2019) study, focussing on apportioning yield by catchment lithology using environmental magnetic tracers and an unmixing model. The sediment yields from the Reinwarth *et al.* (2019) study were used to estimate sediment yield and were subsequently apportioned by lithology using data from the unmixing model.

While environmental magnetic measurements were first used to trace sediment sources in the 1970s (Walling and Oldfield, 1979), the application of sediment source fingerprinting is

fairly recent in South African geomorphological research, and mineral magnetic tracing is most prominent in the fingerprinting literature. There is a research concentration in the Eastern Cape Province, particularly the Karoo region and the Eastern Cape Drakensberg (e.g., Foster *et al.*, 2007; Rowntree and Foster, 2012; van der Waal *et al.*, 2015; Pulley *et al.*, 2015b; Pulley and Rowntree, 2016). The inclusion of (un)mixing models in South African research is also recent (Manjoro *et al.*, 2012; van der Waal, 2014; van der Waal *et al.*, 2015). Lithology formations are frequently used as potential sources when there are different and distinguishable geology units, and there is minimal human influence on erosion rates (D'Haen *et al.*, 2012; Laceby and Olley, 2015) as is the case in the KNP. South African research shows mineral magnetism can successfully distinguish between igneous and sedimentary lithology sources (van der Waal *et al.*, 2015; Pulley and Rowntree, 2016), but has poorer discrimination abilities between shale and sandstone soils (Pulley and Rowntree, 2016). Rowntree *et al.* (2017) use low frequency magnetic susceptibility to discriminate between lithology-based sources to understand sediment source changes in South Africa. Park lithology is a mosaic of igneous, metamorphic, and sedimentary rocks making it a prime study area to assess the ability of mineral magnetism to differentiate between lithology-defined sediment source areas in a near-natural landscape. The cost, speed, and non-destructive method promotes the use of environmental magnetism (Maher, 1998; Dearing, 2000). Furthermore, the success of past magnetic tracing studies in semi-arid South Africa supported its application in the lesser researched savannah landscape of KNP. It is widely acknowledged that magnetic mineralogy is affected by sorting and post-depositional processes and in situ production of minerals (Walden *et al.*, 1997; Foster *et al.*, 2008; Zhang *et al.*, 2008; Wilkinson *et al.*, 2013; Mzuza *et al.*, 2017). Pulley and Rowntree (2016) found the ingrowth of secondary minerals can improve discrimination ability between top- and subsoils, but not between different geology-based sources. The authors also cautioned using magnetism in soils affected by dissolution to trace sediment. There is a lack of systematic research into these uncertainties.

Savannahs are water-limited so sediment and water movement in the landscape is typically episodic, dependant on high magnitude rainfall events (Molles and Cahill, 1999; Hooke, 2003). The high intensity rainfall occurs at the onset of the wet season (between October and April) when vegetation cover is low, leading to high erosion potential (Laker, 2004; Diop *et al.*, 2011). Savannah vegetation is a mosaic of open grasslands and a scatter of woody species (Boughey, 1957; Mati and Veihe, 2001). Vegetation in the Park is controlled by rainfall inputs and influenced by underlying geology (Venter and Gertenbach, 1986, Venter *et al.*,

2003). Woody vegetation cover increases on coarse-grained soils of granite and sandstone landscapes, and grasses dominate the fine-grained soils of basalt and shale plains (Venter *et al.*, 2003; Munyati and Ratshibvumo, 2010). Savannah vegetation plays a vital role in reducing erosion potential, and connectivity, by trapping and storing sediment (Wilcox *et al.*, 1996; Reid *et al.*, 1999; Mati and Veihe, 2001; Cammeraat, 2004; Bartley *et al.*, 2006; Jacobs *et al.*, 2007; Kakembo *et al.*, 2012). Generally, grasses provide a denser ground cover than shrubs and trees and are able to interrupt overland flows and trap and store more eroded material, improve infiltration potential, and strengthen soil and aggregate stability (White, 1979; Toy *et al.*, 2002; Kotzé *et al.*, 2013). The negative relationship between sediment yield and vegetation cover is frequently acknowledged in published literature (Vanmaercke *et al.*, 2014). It can therefore be anticipated that the relationship between vegetation cover and erosion will be transposed on the underlying lithology and will be reflected in sediment yields. Along with vegetation cover and runoff, topography also has a strong control on sediment yield (Vanmaercke *et al.*, 2014). Generally, erosion is worse on steep slopes than gentle slopes because there is greater energy moving water and sediment downslope (Fatunbi and Dube, 2008). In a South African study, gullies and rills most commonly formed on the middle and lower hillslopes (Kakembo *et al.*, 2012). Lower slope areas can be most prone to erosion when poorly vegetated (Bartley *et al.*, 2006; Kakembo *et al.*, 2012). Water is a limited resource in KNP, so the Park management built over 50 small reservoirs to provide additional water sources for wildlife (Pienaar, 1985). The reservoirs led to extensive and severe degradation of vegetation surrounding the reservoirs, creating piospheres (Lange 1969; Brits *et al.*, 2002; Nangula and Oba, 2004; Wessels and Dwyer, 2011). Consequently, many reservoirs were decommissioned. Four of these reservoirs, selected on account of their varied lithology, were used to determine the relative contributions of lithology-defined sources to reservoir sediment and their sediment yields.

2. STUDY AREA

2.1 Background to the KNP

The Kruger National Park lies in north-eastern South Africa, covering an area of almost 20 000 km² and spanning parts of the border with Mozambique (to the east) and Zimbabwe (to the north) (Figure 1). KNP is in the Lowveld Bioregion and is the most extensive savannah-based wildlife reserve in southern Africa (Stewart and Samways, 1998). The topography ranges from flat and undulating plains to hills and low mountains (Venter and Bristow, 1986; Venter *et al.*, 2003). The Lebombo Mountains increase relief along the south-eastern Park

border and form a physical border along the Mozambiquan border. Stream frequency increases with slope (Venter *et al.*, 2003). The study reservoir catchments are in the southern Park and cover a variety of lithology formations (Figure 1). The southern regions are part of the Lowveld Bushveld Zone and receive 500 - 700 mm rainfall per annum (Gertenbach, 1980; Venter *et al.*, 2003).

The unpredictable and unreliable rainfall is a driver of sediment movement in savannahs and determines vegetation composition and abundance. Due to episodic energy entering the system and changes in vegetation cover, connectivity is an important factor in understanding sediment dynamics in these semiarid landscapes.

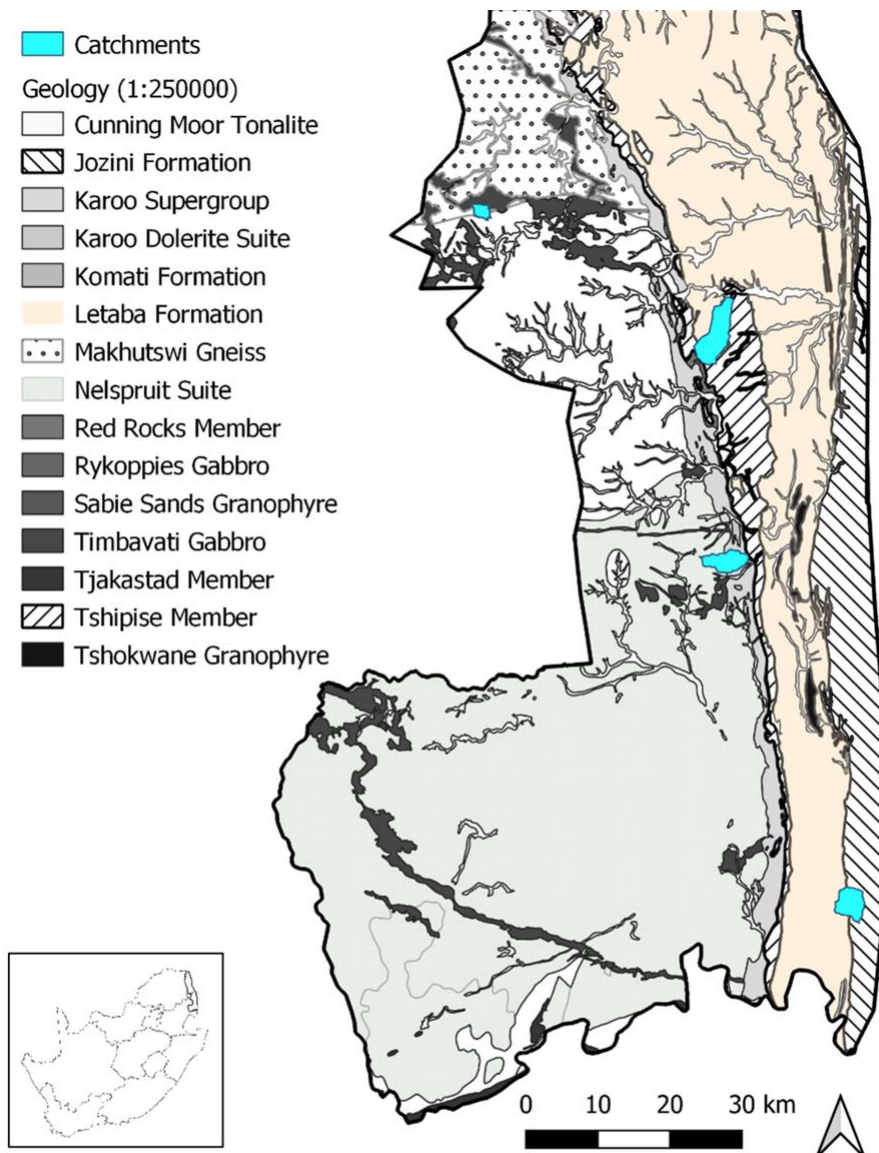


Figure 1: The locality of the Kruger National Park in South Africa (inset) and the study catchments in the lower Park area.

2.1 Sample locations

The Hartbeesfontein catchment lies within undulating plains (~2 % slope) and has an area of 4.3 km² (Figure 1, Table 1). The catchment is underlain by Timbavati Gabbro, Makhutswi Gneiss and Mesoarchaeon Swazian Era Potassic Granite Gneiss (Figure 2). Vegetation cover reflects these soil variations and vegetation density was highest over the gabbro and lowest over the granite gneiss (Venter, 1986; Anhaeusser, 2006). There are wildlife pathways around the reservoir in the granite gneiss lithology (Figure 2). The granite gneiss vegetation was degraded through high utilisation and the creation of a piosphere. Hydrological connectivity is highest in the granite gneiss lithology.

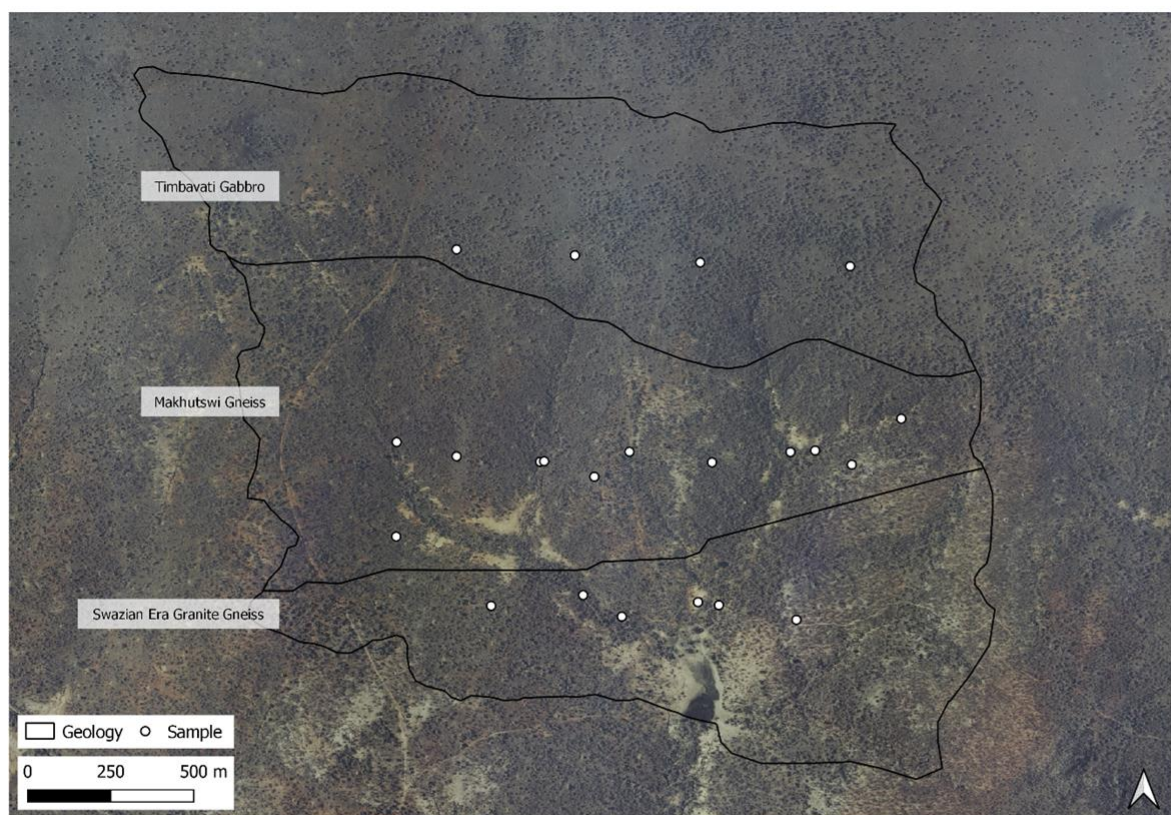


Figure 2: Hartbeesfontein reservoir catchment with sample sites and lithology formation areas (aerial image source: Chief Directorate: National Geo-Spatial Information of South Africa, 2008).

The Marheya catchment (Figure 1) lies within the flat plains (~2 % slope) and has an area of 27.5 km² (Table 1). This catchment is within a low relief landform type, where relief is generally around 10 m (Venter *et al.*, 2003). Letaba River Basalt underlies the central catchment and Clarens Formation sandstone underlies the upper and lower catchment areas (Figure 3). The sandstone soils produced are fine-grained (Venter, 1986; Johnson *et al.* 2006). According to Venter (1986), the basalt soils are easily eroded. Grasses are prevalent over the basalt plains and woody shrub species are more prevalent on the sandstone lithology

(Gertenbach, 1983; Mucina and Rutherford, 2006). Both lithology formations have high hydrological connectivity to the reservoir, which is in the sandstone lithology.

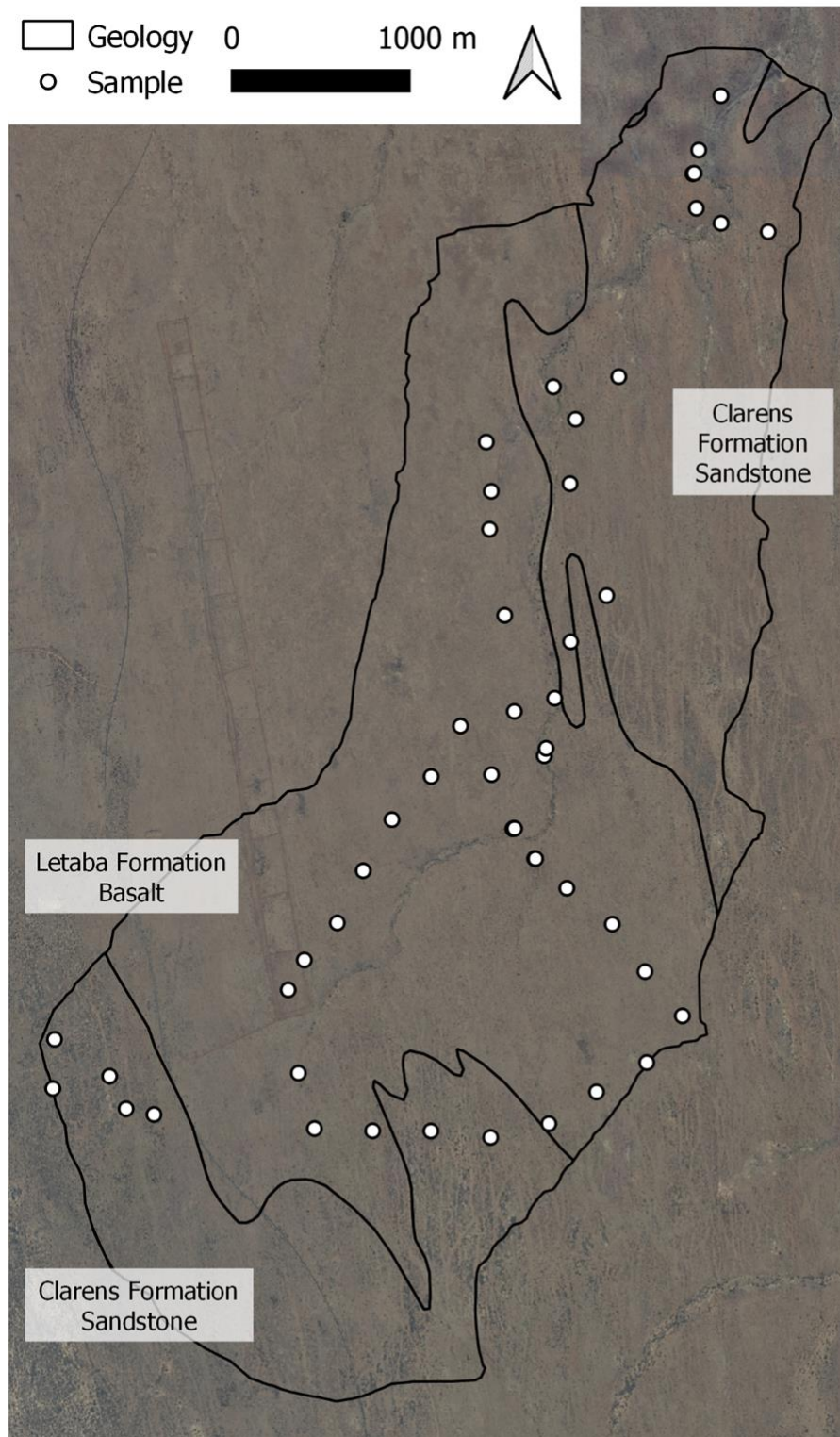


Figure 3: Marheya reservoir catchment with sample sites and lithology formation areas (aerial image source: Chief Directorate: National Geo-Spatial Information of South Africa, 2009).

The Nhlanguzwani catchment (Figure 1) is a combination of low relief and mountain slopes (~4 % slope) and has an area of 16.5 km² (Table 1). The catchment is underlain by Letaba Basalt (flat, low relief) and Jozini Rhyolite (low mountain slopes) (Figure 4). The basalt plains are ~100 m lower than the adjacent rhyolite Lebombo Mountains (Gertenbach, 1983). The basalt lithology and soils are erodible, and the rhyolite lithology is strongly weather resistant and medium grained soils are shallow (Venter, 1986; Duncan and Marsh, 2006). The vegetation is open tree savannah, with dense grass covering the basalt lithology and more woody species over the rhyolite (Gertenbach, 1983; Mucina and Rutherford, 2006). The drainage density is higher over the rhyolite formation. The reservoir is in the basalt lithology and is on the geological border with the rhyolite lithology.

179

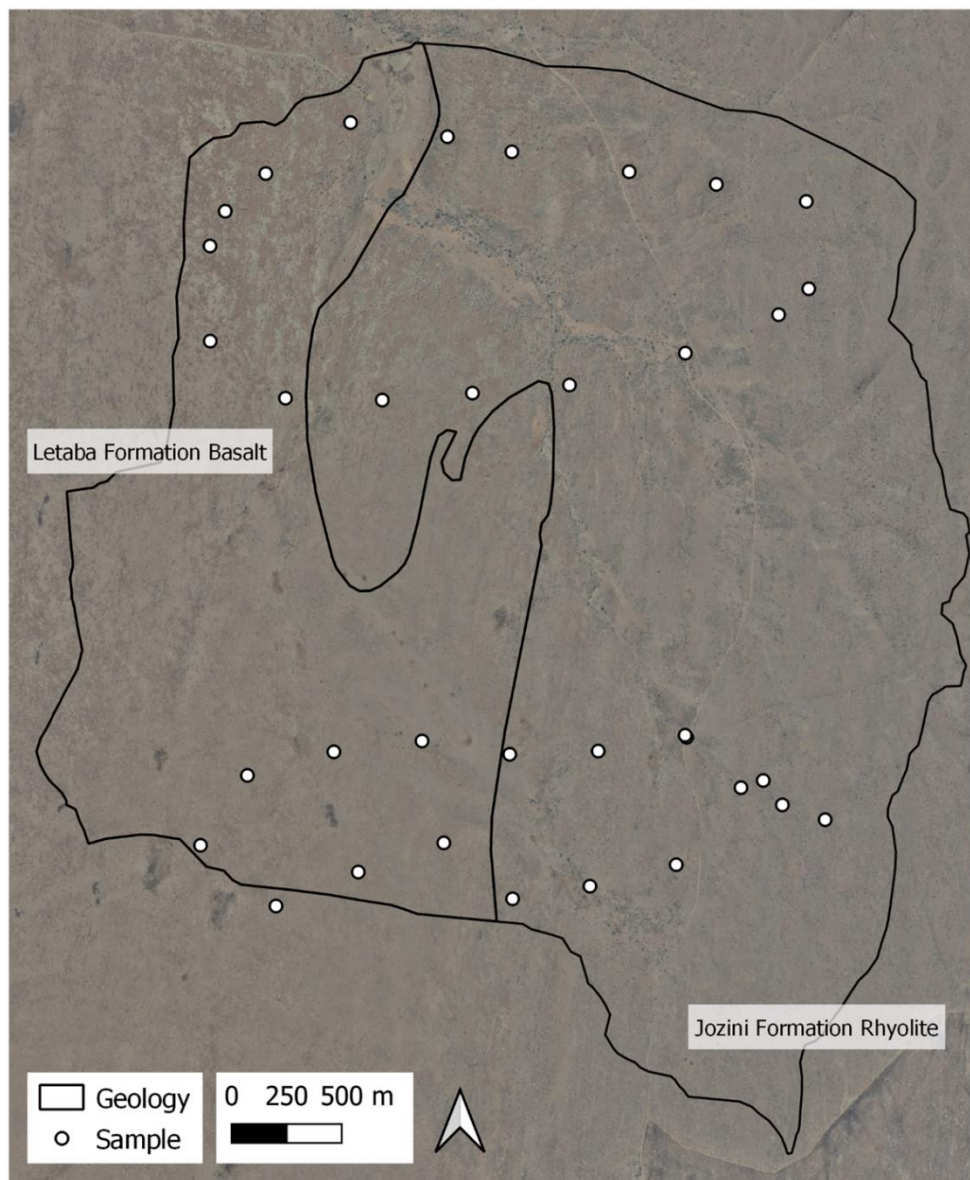


Figure 4: Nhlanguzwani reservoir catchment with sample sites and lithology formation areas (aerial image source: Chief Directorate: National Geo-Spatial Information of South Africa, 2010).

The Silolweni catchment (Figure 1) also lies within the flat plains (~2 % slope) and has an area of 13.2 km² (Table 1). This catchment is within the same low relief landform type as the Marheya catchment. Permian Eccca Group Rocks of the Karoo Supergroup and Nelspruit Suite Granite underlie the catchment (Figure 5). The coarse-grained granite soils are infertile porous sands and easily erodible (Venter, 1986). The Eccca Group duplex soils are also highly erodible (Venter, 1986), with piping common in soils. Woodland is prevalent on the Eccca Formation shales and thicket vegetation is dominant on the sandy granite soils (Gertenbach, 1983; Mucina and Rutherford, 2006). The main river crosses the length of the catchment, and gully systems were noted in both lithologies. Figure 6 shows the progression of gully formation in the Eccca Group lithology. The gully formations increase connectivity potential. The Nhlangezani and Silolweni reservoirs were decommissioned in 2008 and 2007 respectively because of severe eutrophication (SANParks, 2008; Baade *et al.*, 2012).

Table 1: Catchment information: area, slope, lithology and lithology area, number of samples collected per lithology, catchment and lithology potential drainage density, and catchment specific sediment yield.

Catchment	Area (km ²) ¹	Mean Slope (%) ¹	Lithology and lithology area (%) ²	Samples collected per lithology	Catchment PDD (km km ⁻²)	Catchment lithology PDD (km km ⁻²)	SSY (t km ⁻² yr ⁻¹) ²
Hartbeesfontein	4.3	2.4 ± 1.1	Gabbro (35 %) Gneiss (38 %) Granite gneiss (27 %)	4 12 6	1.35	Gabbro 0.24 Gneiss 2.61 Granite gneiss 1.03	55 ± 8
Marheya	27.5	1.8 ± 0.8	Basalt (54 %) Sandstone (46 %)	33 21	1.31	Basalt 1.16 Sandstone 0.95	8 ± 2
Nhlanganzwani	16.5	3.9 ± 4.7	Basalt (50 %) Rhyolite (50%)	12 21	0.88	Basalt 0.24 Rhyolite 0.76	35 ± 4
Silolweni	13.2	1.9 ± 1.0	Ecca Group (54 %) Granite (46 %)	34 31	0.74	Ecca Group 0.56 Granite 0.45	62 ± 8

¹Baade and Schmulius (2015); ²Reinwarth *et al.* (2018); PDD: potential drainage density; SSY: specific sediment yield

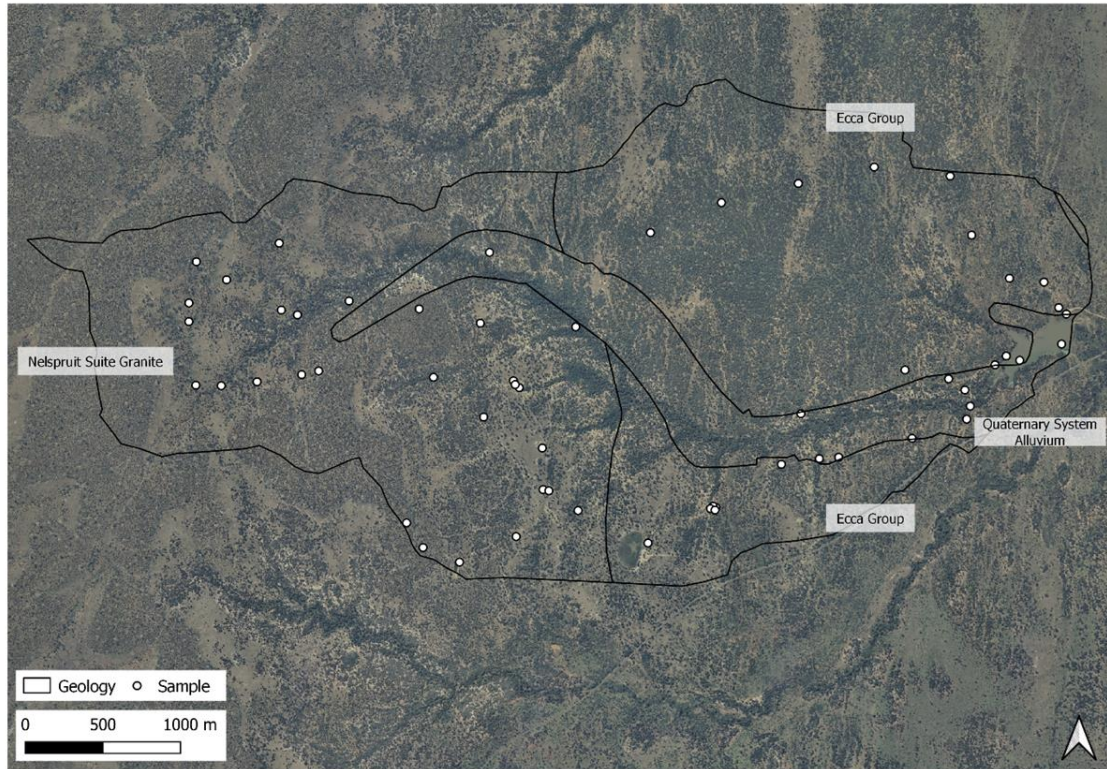


Figure 5: Silolweni reservoir catchment with sample sites and lithology formation areas (aerial image source: Chief Directorate: National Geo-Spatial Information of South Africa, 2009).

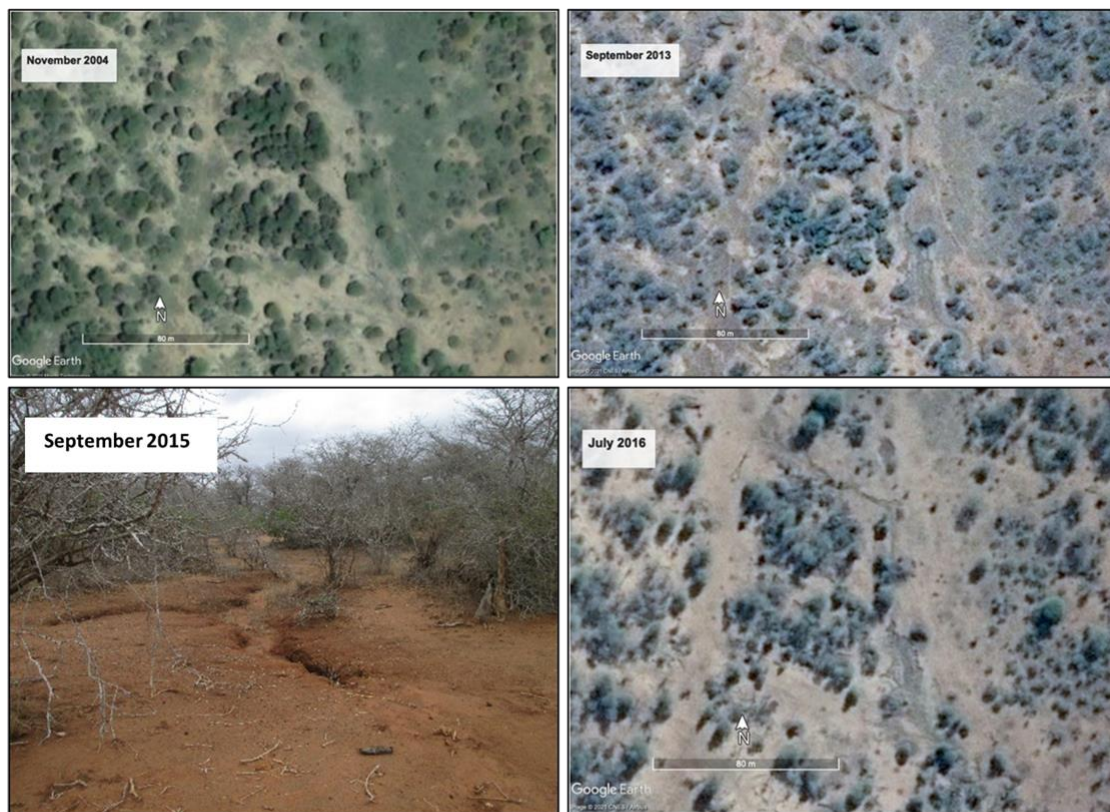


Figure 6: Gully formation over time (Source: Google Earth and field photograph).

3. MATERIALS AND METHODS

This section describes the field sampling, laboratory, and statistical methods used to determine sediment yields. Catchment area (Baade and Schmulius, 2015) and lithology area percentages (Reinwarth *et al.*, 2018) were established from published literature. Catchment lithologies were the sources identified for the fingerprinting method. Potential drainage density measured visible river channels (longitudinal connectivity) on colour aerial photographs taken in 2008-2010, sourced from the Chief Directorate: National Geo-Spatial Information (NGI) of South Africa, using Geographic Information Systems (GIS).

3.1 Field Sampling

Field campaigns took place in 2014 (all catchments) and 2015 (Marheya and Silolweni) and logistics included obtaining a general research permit for the Park and permission from Park Section Rangers to enter and sample catchments, and an appointed game guard armed with an elephant rifle was also present in the field. Wildlife pathways were used to move through the bush more easily and samples were taken approximately three metres away from the trail to minimise disturbance (van der Waal, 2014). Movements within the Nhlanguzani catchment were restricted after the second sampling day because of anti-game-poaching activities. Access to Nhlanguzani and Hartbeesfontein catchments was denied for the same reason in 2015, resulting in the low numbers of catchment samples collected in Hartbeesfontein.

Catchment sampling was flexible, and routes were semi-structured because random sampling on foot was not practical in the zoologically dangerous terrain. The circular sampling routes were closed (beginning and ending at the vehicle) to limit time in the field and avoid risk. The number of samples and their distribution between lithologies is provided in Table 1. The samples were ascribed lithologies based on the geological map. Surface samples of 10 cm depth were collected in each mapped catchment lithology using a 2.5 cm diameter stainless steel corer, following the procedures outlined by van der Waal (2014) and Pulley *et al.* (2015b). Samples were taken halfway down the gully wall in the Silolweni catchment following the method of van der Waal (2014). One reservoir core was taken at a point of assumed deepest sediment using an Eijkelkamp percussion corer. Reservoir depth information was received on-site from another research team, data published in Reinwarth *et al.* (2018). The boundary between deposit and reservoir bottom was determined by colour and particle size changes (Baade *et al.* 2012; Reinwarth *et al.*, 2017; Reinwarth *et al.*, 2018).

3.2 Laboratory Analyses

Sample material was oven dried at 40 °C to prevent alteration of mineral magnetic signatures at high temperatures (Dearing 1999) and gently disaggregated using a pestle and mortar. Reservoir cores were sectioned at 2 cm intervals and were treated in the same way as the source sample material. The common practice of using the <63 µm fraction (Olley and Caitcheon, 2000; Hatfield and Maher, 2009; Pulley *et al.*, 2015b) in fingerprinting studies was not applied in this study because most of the sediment was in the 125 – 500 µm particle size range. The <63 µm fraction accounted for only 10 – 19 % of catchment and 7 -17 % of reservoir sediment. Therefore, material was mechanically dry sieved to <500 µm particle size fraction. Descriptions of sample material include sand, silt, clay (Friedman and Sanders, 1978; Blott and Pye, 2001). Mineral magnetic measurements were made using 8 - 10 g of material sealed into 10 ml sample pots. Measurements of the mineral magnetic signatures followed the procedures outlined by Maher (1986), Walden (1999), Dearing (1999), Lees (1997), Foster *et al.* (2007) and Pulley *et al.* (2015a). The measured parameters and instrumentation used are given in Table 2. Organic matter content was determined using approximately 5 g of sample material heated in a Carbolite muffle furnace at 450 °C for 4 hours (Grimshaw, 1989; Pulley *et al.*, 2015a).

3.3 Statistical Analyses

The sediment source fingerprinting analysis followed the methods of Collins *et al.* (1997a), McKinley *et al.* (2013), and Pulley *et al.* (2015a). The Mann-Whitney U and Kruskal-Wallis H tests showed whether significant differences existed between the magnetic signatures of the potential catchment sources (p-value = 0.05). A mass conservation test identified tracers that showed non-conservatism, i.e., when 80 % or more reservoir samples were within the defined range of the source medians (Wilkinson *et al.*, 2013, Pulley *et al.*, 2015a, Kraushaar *et al.*, 2015). The tracers that showed significant differences and conservative behaviour were included in a Discriminant Function Analysis, which identified tracer combinations of optimum source discrimination ability. An accuracy percentage of 80 % was chosen for the tracer combination to be used in the modelling process. This threshold minimises potential uncertainty produced by source discrimination and has been used as a guide value by Pulley *et al.* (2015a).

Table 2: Parameters measured and derived during mineral magnetic analysis (Maher, 1986; Walden, 1999; Dearing, 1999; Lees, 1997; Foster *et al.*, 2007; Pulley *et al.*, 2015a).

Parameter	Unit	Measured (M) or Derived (D)	Measured minerals	Instrument or equation
Magnetic Susceptibility				
Low frequency Susceptibility (χ_{lf})	$10^{-6} \text{ m}^3 \text{ kg}^{-1}$	M	Diamagnetic, paramagnetic, canted antiferromagnetic, ferrimagnetic	Bartington Instruments® MS2 meter and MS2 dual-frequency sensor (470 Hz)
High frequency susceptibility (χ_{hf})	$10^{-6} \text{ m}^3 \text{ kg}^{-1}$	M		Bartington Instruments® MS2 meter and MS2 dual-frequency sensor (4700 Hz)
Frequency dependent susceptibility (χ_{fd})	$10^{-9} \text{ m}^3 \text{ kg}^{-1}$	D	Ultrafine super paramagnetic, semi-quantitative measure of super paramagnetic grains	$((\chi_{lf} - \chi_{hf})/m) * 100$ (where m = sample mass)
Magnetic Remanence				
Anhyseretic Remanent Magnetization ($ARM_{(40\mu m)}$)	$10^{-3} \text{ Am}^2 \text{ kg}^{-1}$	M	Stable single domain ferrimagnetic	Molspin® A. F. Magnetiser with ARM att. Molspin® Rotating Magnetometer
Susceptibility of ARM (χ_{arm})	$10^{-6} \text{ m}^3 \text{ kg}^{-1}$	D	Stable single domain ferrimagnetic	$ARM \times 3.14 \times 10$
Saturation Isothermal Remanent Magnetisation (SIRM)	$10^{-3} \text{ Am}^2 \text{ kg}^{-1}$	M	Minerals carrying remanence	Molspin® Pulse Magnetiser Molspin® Rotating Magnetometer
Soft Isothermal Remanent Magnetisation ($IRM_{(-1000 \text{ mT})}$)	$10^{-3} \text{ Am}^2 \text{ kg}^{-1}$	M		Molspin® Pulse Magnetiser Molspin® Rotating Magnetometer
S-ratio	-	D		$-1 \times (IRM_{100mT} / IRM_{1.0T})$
Hard Isothermal Remanent Magnetisation (HIRM)	$10^{-3} \text{ Am}^2 \text{ kg}^{-1}$	D	Antiferromagnetic	$IRM_{1T} / (1 - S\text{-ratio}) / 2$

The unmixing model used was developed by Pulley *et al.* (2015a) which included Monte Carlo uncertainty analysis. Each reservoir core sample was modelled for 1000 iterations (Collins and Walling, 2007), based on the median deviation of source signatures. The inclusion of Monte Carlo uncertainty analysis also means the goodness of fit is not the only determinant of model robustness (Pulley, 2014). The 25th and 75th percentile model estimates indicate the range of uncertainty in the results (Janssen, 2013; Pulley, 2014). The range provides insight into the variability of estimates, where higher variability in source estimates down the core means a wider percentile range.

The specific sediment yields for each lithology were estimated using the total catchment sediment yields ($\text{t km}^{-2} \text{ yr}^{-1}$) published by Reinwarth *et al.* (2019), the source (lithology) contribution estimates of the (un)mixing models (%), and the mapped lithology area (%). The estimated source contributions were used to approximate the sediment yield per lithology.

Sediment Yield by Lithology Calculation

$$\frac{\text{lithology contribution estimate (\%)}}{\text{lithology area (\%)}} \times \text{catchment specific sediment yield}$$

4. RESULTS

This section presents source sample characteristics, downcore changes and modelling source contributions, and sediment yields by lithology estimates for each catchment. The findings are summarised in the discussion and conclusion.

4.1 Hartbeesfontein Catchment

The sample numbers were low for this catchment and access to the catchment for continued was denied because of anti-game-poaching activities. The gabbro soils were fine to medium sand, and the gneiss and granite gneiss soils were medium sand. The Kruskal-Wallis H test showed no statistically significant differences in particle size between the three sources (p-value = 0.08), but the Mann Whitney U-test showed a significant difference in particle size between the gabbro and granite gneiss sources (p-value = 0.01). The organic matter content was highest in the gabbro soil (~12%) and lowest in the granite gneiss soils (+2 %). The gabbro mineral magnetic signatures were highest of the sources and the granite gneiss signatures were the lowest (Table 3). The Kruskal-Wallis H test showed statistically significant differences in mineral magnetic tracers between the three sources (Table 4). The only statistical comparison using the Mann Whitney U-test that showed no significant

differences was between the gneiss and granite gneiss $\chi_{fd_{min}}$ tracer signatures (p-value = 0.6) (Table 4).

Downcore plots showed notable changes in the median particle size (coarsening of particle sizes) and mineral magnetic signatures (decreasing signatures in $\chi_{lf_{min}}$ and χ_{arm}) at ~40 cm depth (Figure 4). These changes are indicative of potential dissolution of very-fine grained magnetic minerals below ~40 cm depth (Figure 7). Organic matter content varied down the core, with a range of 2 – 5 %. The median χ_{arm} / SIRM ratio value of ~10 was greater than 2 suggesting the likely presence of bacterial magnetite. Bacterial magnetite was also indicated in all source material.

The $\chi_{lf_{min}}$ and HIRM tracers passed the mass conservation test in the analysis of the full core. Conversely, the $\chi_{lf_{min}}$, $\chi_{fd_{min}}$, SIRM and HIRM tracers passed the test only in the upper 40 cm of the core. These results indicated non-conservatism of signatures in the core below 40 cm depth. Consequently, only the upper 40 cm was analysed. The $\chi_{lf_{min}}$, $\chi_{fd_{min}}$, SIRM and HIRM tracer combination had a 100 % source discrimination accuracy and were used in the modelling process. The (un)mixing model estimated 100+0 % contribution from the granite gneiss source, despite this lithology covering the smallest catchment area.

Table 3: The median and median absolute deviations (MAD) of tracer signatures for the Hartbeesfontein catchment sources.

Sources		Tracers				
		$\chi_{lf_{min}}$ ($10^{-6}m^3kg^{-1}$)	$\chi_{fd_{min}}$ ($10^{-6}m^3kg^{-1}$)	χ_{arm} ($10^{-6}m^3kg^{-1}$)	SIRM ($10^{-3}Am^2kg^{-1}$)	HIRM ($10^{-3}Am^2kg^{-1}$)
Gabbro	Median	2.25	150.10	20.30	2.37	2.12
	MAD	0.15	7.67	0.22	0.17	0.17
Gneiss	Median	0.83	48.83	9.81	1.22	0.96
	MAD	0.10	20.37	1.98	0.16	0.23
Granite gneiss	Median	0.28	17.45	5.08	0.54	0.40
	MAD	0.08	6.75	1.23	0.18	0.09

Table 4: The Mann-Whitney U (two sources) and the Kruskal-Wallis H (three sources) test results comparing source tracer signatures in the Hartbeesfontein catchment ($\alpha = 0.05$).

	Gabbro vs Gneiss	Gabbro vs Granite gneiss	Gneiss vs Granite gneiss	Gabbro vs Gneiss vs Granite gneiss
$\chi_{lf_{min}} (10^{-6} \text{ m}^3 \text{ kg}^{-1})$				
p-value	<0.01	0.01	<0.01	<0.01
Significant	Yes	Yes	Yes	Yes
$\chi_{fd_{min}} (10^{-6} \text{ m}^3 \text{ kg}^{-1})$				
p-value	<0.01	0.01	0.6	<0.01
Significant	Yes	Yes	No	Yes
$\chi_{arm} (10^{-6} \text{ m}^3 \text{ kg}^{-1})$				
p-value	0.01	0.01	0.03	<0.01
Significant	Yes	Yes	Yes	Yes
SIRM ($10^{-3} \text{ Am}^2 \text{ kg}^{-1}$)				
p-value	<0.01	0.01	0.01	<0.01
Significant	Yes	Yes	Yes	Yes
HIRM ($10^{-3} \text{ Am}^2 \text{ kg}^{-1}$)				
p-value	<0.01	<0.01	<0.01	<0.01
Significant	Yes	Yes	Yes	Yes

'Yes' indicates significant differences; 'No' indicates no significant differences

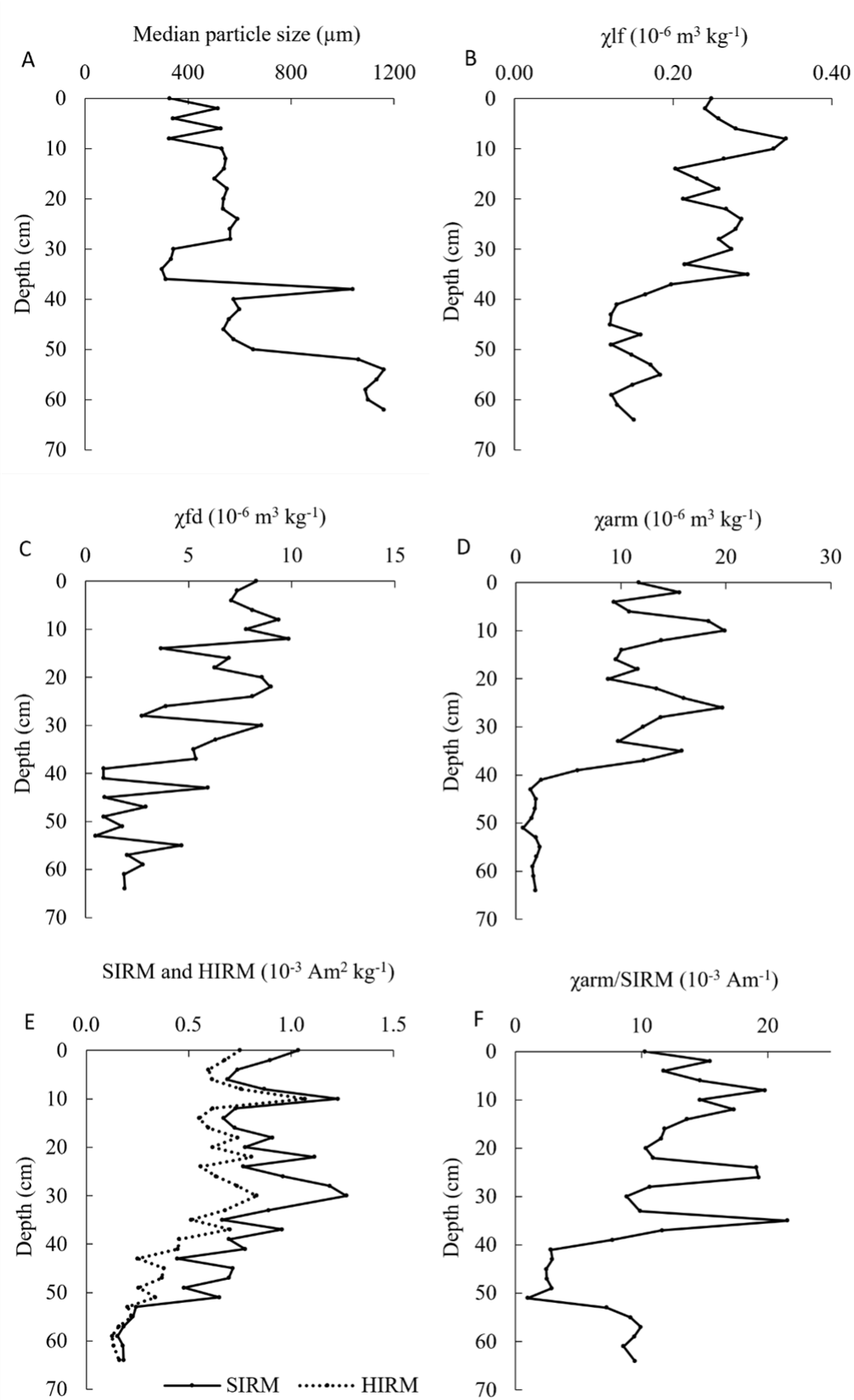


Figure 7: Hartbeesfontein reservoir downcore plots of median particle size (A), magnetic signatures of $\chi_{lf_{min}}$ (B), χ_{fd} (C), χ_{arm} (D), SIRM and HIRM (E) parameters and χ_{arm}/SIRM (F) ratio.

Reinwarth *et al.* (2019) estimated a sediment yield of $55 \text{ t km}^{-2} \text{ yr}^{-1}$ for the entire catchment. Adjusting for the smaller area of the granite gneiss that contributed an estimated 100% of the sediment, the estimated sediment yield of the granite gneiss source was $204 \text{ t km}^{-2} \text{ yr}^{-1}$. The reservoir is in the granite gneiss lithology and there were large areas of sparse vegetation and exposed soils surrounding the reservoir, as well as game tracks leading to the reservoir (Figure 2). Therefore, the distance for and energy required to transport eroded material to reach the reservoir was low and the game tracks provided a high degree of connectivity.

4.2 Marheya Catchment

The basalt soils were fine sand and the sandstone soils were very fine sand. The median particle sizes of the two sources were compared using the Mann-Whitney U test and statistically significant differences were found (p -value = 0.001). The basalt soils contained double the amount of organic matter (~6 %) than the sandstone soils (~3 %). Mineral magnetic signatures were higher for the basalt soils than the sandstone soils. Statistical comparison of the signatures showed significant differences in the $\chi_{lf_{min}}$, χ_{arm} , SIRM and HIRM tracers but not between the $\chi_{fd_{min}}$ signatures (p -value = 0.11) (Table 5).

Table 5: The median and median absolute deviations (MAD) of tracer signatures for the Marheya catchment sources, and the Mann-Whitney U test comparisons.

Sources		Tracers				
		$\chi_{lf_{min}}$ ($10^{-6} \text{ m}^3 \text{ kg}^{-1}$)	$\chi_{fd_{min}}$ ($10^{-6} \text{ m}^3 \text{ kg}^{-1}$)	χ_{arm} ($10^{-6} \text{ m}^3 \text{ kg}^{-1}$)	SIRM ($10^{-3} \text{ Am}^2 \text{ kg}^{-1}$)	HIRM ($10^{-3} \text{ Am}^2 \text{ kg}^{-1}$)
Basalt	Median	3.90	137.74	58.29	0.96	0.76
	MAD	1.15	21.43	13.50	0.14	0.09
SS	Median	2.92	116.28	40.92	0.53	0.47
	MAD	1.19	43.51	17.50	0.07	0.11
MWU	p-value	<0.01	0.11	<0.01	<0.01	<0.01
	Sig.	Yes	No	Yes	Yes	Yes

SS: sandstone; MWU: Mann-Whitney U test; sig: significant

‘Yes’ indicates significant differences; ‘No’ indicates no significant differences

There was a fining of sediment in the upper ~26 cm of the core and changes in particle size at ~50 cm (Figure 5). Organic matter content increased up the core, with content peaking in the upper ~20 cm of the core. Downcore plots showed the least variation in mineral magnetic signatures in the upper ~20 cm (Figure 8). Bacterial magnetite ingrowth was suggested in both the source material and the reservoir core (median χ_{arm} / SIRM ratio: ~35).

The $\chi_{lf_{min}}$, χ_{arm} , and SIRM tracers passed the Mass Conservation Test, and the tracer combination had an 89 % source discriminant accuracy. The (un)mixing model estimated a 66 \pm 30 % contribution from the sandstone and a 34 \pm 30 % contribution from the basalt lithology (Table 5). Downcore estimates suggested cyclical changes in the dominant source, with basalt contributing as much as 75 % of sediment to the reservoir sediment at times (Figure 9). The variation in source estimates accounted for the wide sample median range and high uncertainty range indicated by percentiles (Table 6).

The Marheya catchment has an estimated sediment yield of 8 t km⁻² yr⁻¹ (Reinwarth *et al.*, 2019). The sandstone lithology covered 46 % of the catchment area and the estimated sediment yield was 11 t km⁻² yr⁻¹. The estimated sediment yield of the basalt lithology to the reservoir was 5 t km⁻² yr⁻¹. The reservoir was in the sandstone lithology and the basalt lithology covered the central catchment area, further from the reservoir so eroded sediment had a greater travel distance.

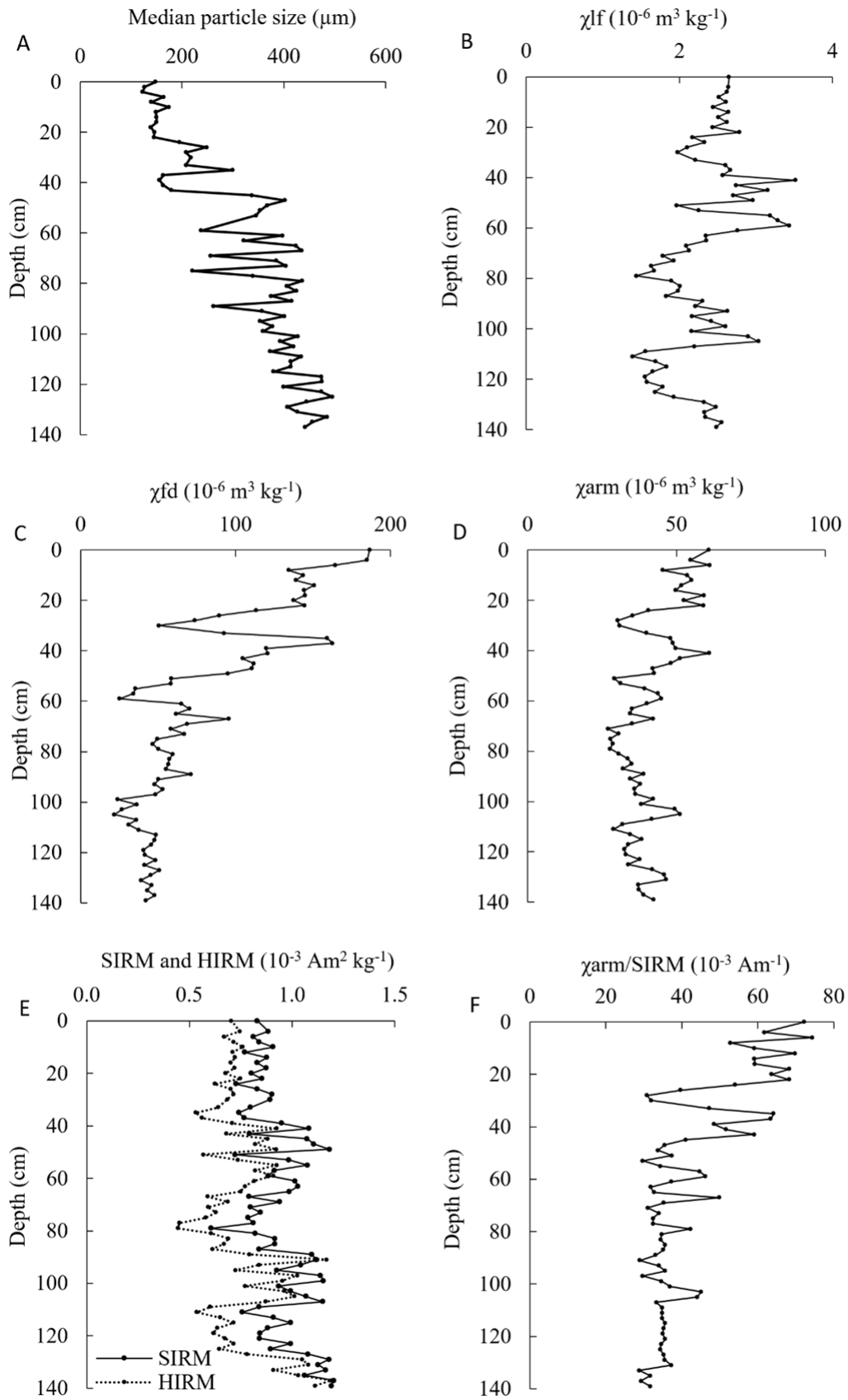


Figure 8: Marheya reservoir downcore plots of median particle size (A), magnetic signatures of $\chi_{lf_{\min}}$ (B), χ_{fd} (C), χ_{arm} (D), SIRM and HIRM (E) parameters and χ_{arm}/SIRM (F) ratio.

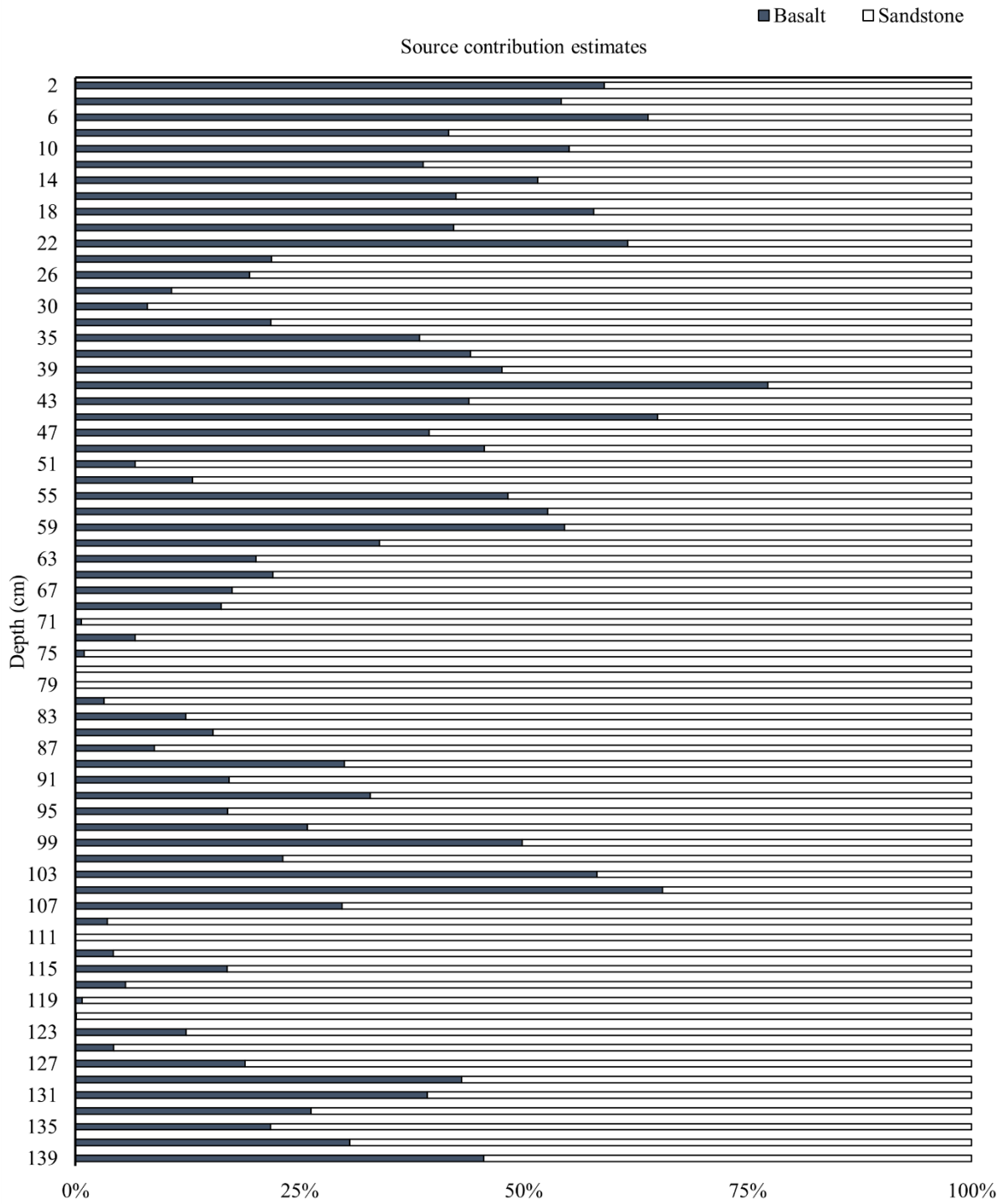


Figure 9: Median estimated contributions of the Marheya sources to reservoir sediment.

Table 6: The (un)mixing model source contribution estimates (%) to the Marheya reservoir sediment.

Source	Summary values for the core				Downcore variability		
	Median	Percentile range (25% - 75%)	Uncertainty (75% - 25%)	Median goodness of fit (%) [range]	Sample median range	Sample percentile range (25% - 75%)	Median sample uncertainty [range]
Basalt	34	16 – 46	30	85	0 – 92	4 – 93	74
Sandstone	66	54 – 84		[49 -55]	8 – 100	7 – 96	[49 -95]

4.3 Nhlangezani Catchment

The rhyolite soils were medium sand, and the basalt soils were fine sand. The Mann-Whitney U test, however, showed no statistically significant differences in median particle size between these potential sources (p-value = 0.3). The organic matter content was relatively high for this study in both the basalt (~13 %) and rhyolite (~11 %) soils. In general, the basalt magnetic signatures were higher than the rhyolite. Statistical comparison of the signatures showed significant differences in the $\chi_{fd_{min}}$, χ_{arm} , SIRM and HIRM tracers but not between the $\chi_{lf_{min}}$ signatures (p-value = 0.11) (Table 7).

Table 7: The median and median absolute deviations (MAD) of tracer signatures for the Nhlangezani catchment sources.

Sources		Tracers				
		$\chi_{lf_{min}}$ ($10^{-6} \text{ m}^3 \text{ kg}^{-1}$)	$\chi_{fd_{min}}$ ($10^{-6} \text{ m}^3 \text{ kg}^{-1}$)	χ_{arm} ($10^{-6} \text{ m}^3 \text{ kg}^{-1}$)	SIRM ($10^{-3} \text{ Am}^2 \text{ kg}^{-1}$)	HIRM ($10^{-3} \text{ Am}^2 \text{ kg}^{-1}$)
Bas	Median	4.80	421.34	70.14	0.87	0.52
	MAD	0.91	225.72	13.19	0.07	0.04
Rhy	Median	4.22	143.66	22.09	0.54	0.31
	MAD	1.19	109.27	8.61	0.15	0.07
MWU	p-value	0.11	0.00	0.00	0.00	0.00
	Sig.	No	Yes	Yes	Yes	Yes

Rhy: rhyolite; MWU: Mann-Whitney U test; sig: significant

'Yes' indicates significant differences; 'No' indicates no significant differences

Downcore plots showed three major peaks in particle size in the upper ~20 cm of the core (Figure 10), likely indicating flood events that transported coarse sediment to the reservoir. The uppermost 30 cm of the core had higher organic matter content than the rest of the core. This is likely due to the blue/green algal bloom that led to the reservoir decommissioning in 2007. After the decommissioning, vegetation was able to colonise the reservoir area. There

was bacterial magnetite ingrowth in both source material and the reservoir core (median χ_{arm} / SIRM ratio: ~ 86).

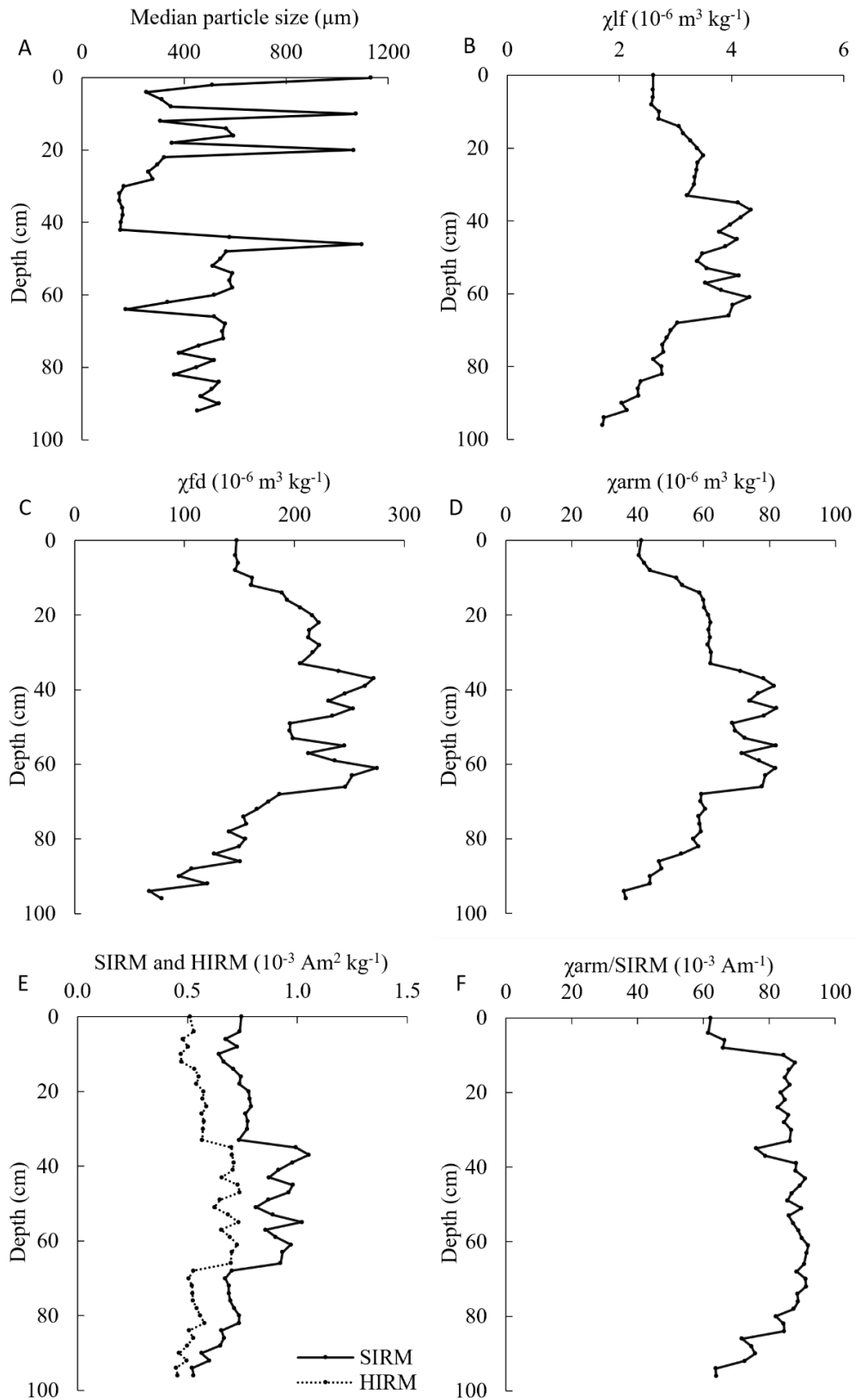


Figure 10: Nhlangezani reservoir downcore plots of median particle size (A), magnetic signatures of $\chi_{lf_{min}}$ (B), χ_{fd} (C), χ_{arm} (D), SIRM and HIRM (E) parameters and χ_{arm}/SIRM ratio.

The $\chi_{fd_{min}}$, χ_{arm} , SIRM tracers passed the Mass Conservation Test and had a 98 % source discriminant accuracy. The (un)mixing model estimated a 70 \pm 26 % contribution from the rhyolite lithology (Table 8). The downcore estimates show downcore variability in source contributions, with peaks in basalt contributions in the central core section (Figure 11). The uncertainty range per sample derived from model iterations was high, which indicates multi-source contributions (Table 8).

Reinwarth *et al.* (2019) estimated a sediment yield of 35 t km⁻² yr⁻¹ for the entire catchment. Each source covered 50 % of the catchment area. The estimated sediment yield to the reservoir of the rhyolite was 50 t km⁻² yr⁻¹ and 20 t km⁻² yr⁻¹ for the basalt lithology. The reservoir was in the basalt lithology, on the geological border of the rhyolite lithology. The slope and drainage network density were higher for the rhyolite source.

Table 8: The (un)mixing model source contribution estimates (%) to the Nhlanguzwani reservoir sediment.

Source	Summary values for the core				Downcore variability		
	Median	Percentile range (25% - 75%)	Uncertainty (75% - 25%)	Median goodness of fit (%) [range]	Sample median range	Sample percentile range (25% - 75%)	Median sample uncertainty [range]
Basalt	30	19 - 45	26	84 [42 - 97]	0 - 54	0 - 97	54 [5 - 92]
Rhyolite	70	55 - 81			46 - 100	3 - 100	

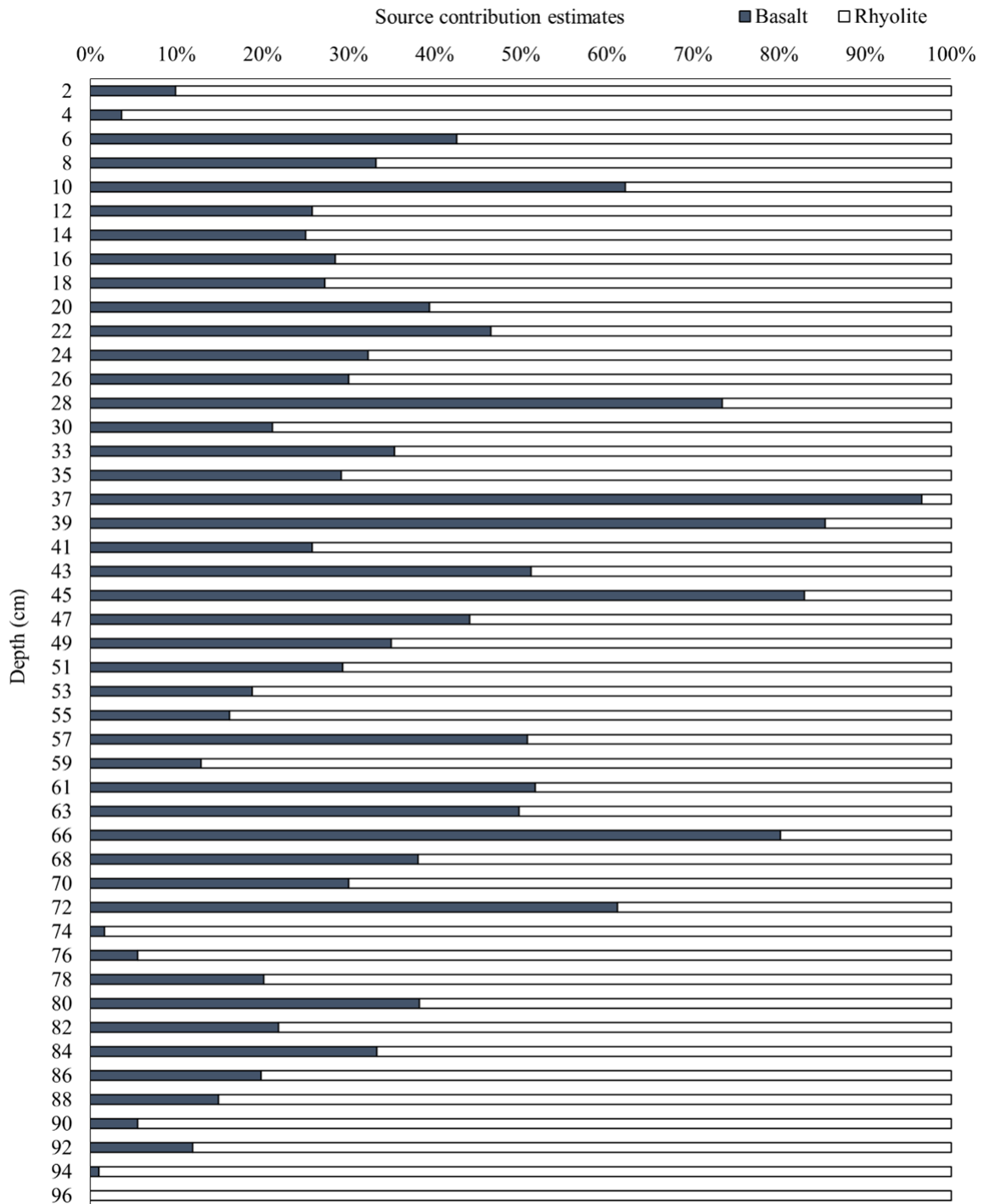


Figure 11: Median estimated contributions of the Nhlangezani sources.

4.4 Silolweni Catchment

The Ecga Group and granite soils were medium sand. The Mann-Whitney U test showed no statistically significant differences between the source particle sizes (p-value = 0.11). The organic matter content was similar in the Ecga Group (~3 %) and granite (~2 %) soils. The Mann-Whitney test showed statistically significant differences between source signatures of

the $\chi_{lf_{min}}$, $\chi_{fd_{min}}$, χ_{arm} tracers, but not for the SIRM (p-value = 0.76) and HIRM (p-value = 0.99) tracers (Table 9).

Table 9: The median and median absolute deviations (MAD) of tracer signatures for the Silolweni catchment sources.

Sources		Tracers				
		$\chi_{lf_{min}}$ ($10^{-6} \text{ m}^3 \text{ kg}^{-1}$)	$\chi_{fd_{min}}$ ($10^{-6} \text{ m}^3 \text{ kg}^{-1}$)	χ_{arm} ($10^{-6} \text{ m}^3 \text{ kg}^{-1}$)	SIRM ($10^{-3} \text{ Am}^2 \text{ kg}^{-1}$)	HIRM ($10^{-3} \text{ Am}^2 \text{ kg}^{-1}$)
Ecca Group	Median	0.36	26.61	29.43	0.54	0.42
	MAD	0.09	8.72	9.01	0.10	0.07
Granite	Median	0.22	10.82	20.28	0.50	0.39
	MAD	0.07	4.40	3.69	0.07	0.06
MWU	p-value	0.00	0.00	0.00	0.76	0.99
	Sig.	Yes	Yes	Yes	No	No

MWU: Mann-Whitney U test; sig: significant

'Yes' indicates significant differences; 'No' indicates no significant differences

The median particle size down the Silolweni reservoir core was quite homogeneous, except for two major peaks in particle size (Figure 9). The Silolweni reservoir was also decommissioned because of high eutrophication. Organic matter content was highest in the upper ~10 cm of the core, which could be attributed to vegetation colonisation and growth since decommissioning. The $\chi_{lf_{min}}$ and χ_{arm} signature patterns down the core showed low variation, apart from the increase in $\chi_{lf_{min}}$ values in the upper ~10 cm of the core (Figure 12). Bacterial magnetite ingrowth was shown in the reservoir core (median χ_{arm} / SIRM ratio: ~46).

The $\chi_{lf_{min}}$, $\chi_{fd_{min}}$, χ_{arm} tracers passed the Mass Conservation Test and had a 74 % source discriminant accuracy. The (un)mixing model estimated a 77+-19 % contribution from the granite lithology (Table 10), but downcore estimates showed close to 100 % contribution from the Ecca Group source in the upper ~10 cm of the core (Figure 13). This Ecca Group contribution was reflected in the change of $\chi_{lf_{min}}$ signatures in this core section.

The Silolweni catchment had an estimated sediment yield of $62 \text{ t km}^{-2} \text{ yr}^{-1}$ (Reinwarth *et al.*, 2019). The granite lithology covers 46 % of the catchment, and the estimated sediment yield was $123 \text{ t km}^{-2} \text{ yr}^{-1}$. In comparison, the estimated sediment yield of the Ecca Group lithology was $10 \text{ t km}^{-2} \text{ yr}^{-1}$. Although the granite lithology is furthest from the reservoir, the estimated sediment yield of this source to the reservoir was 10 times greater than that estimated for the Ecca Group lithology.

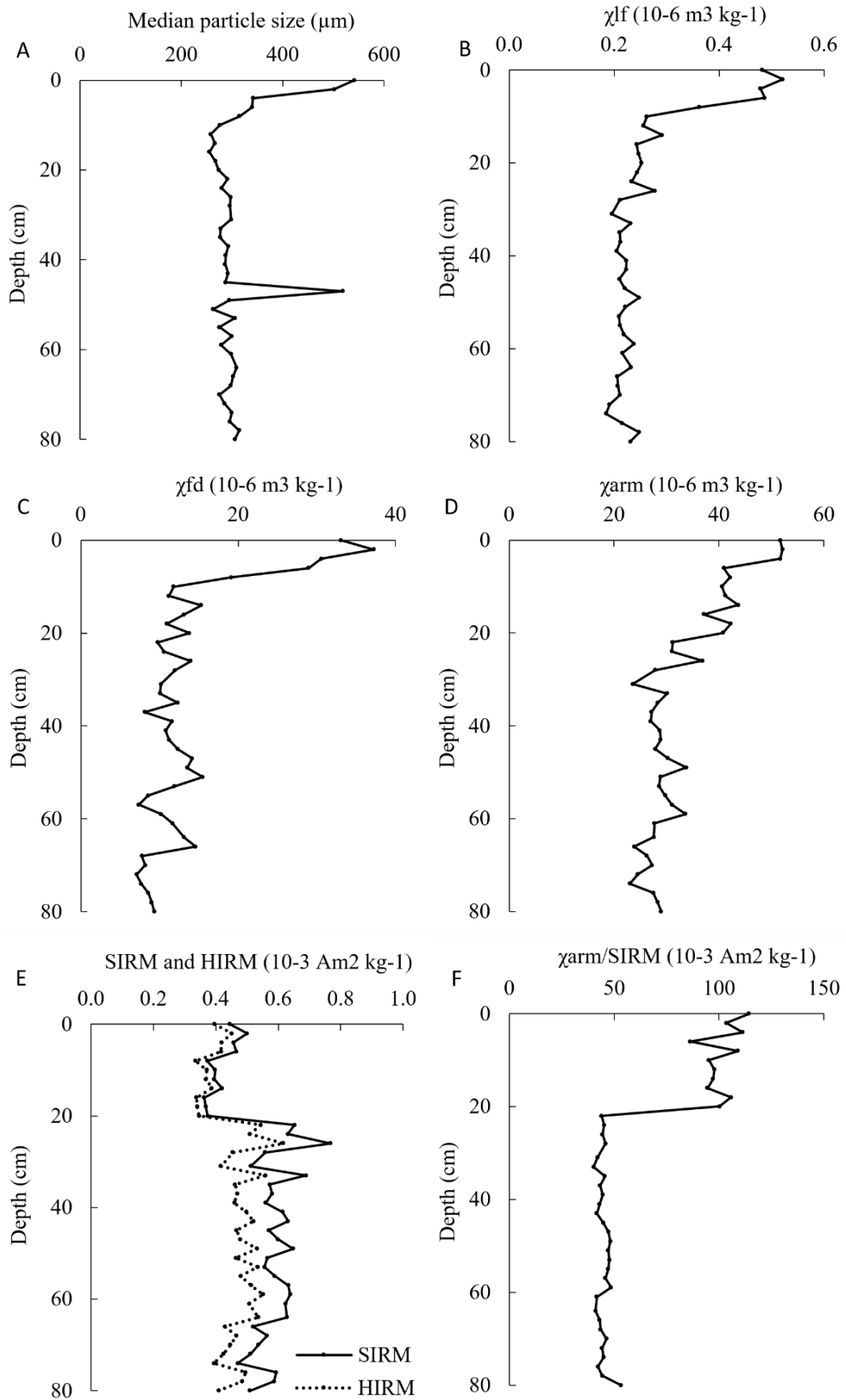


Figure 12: Silolweni reservoir downcore plots of median particle size (A), magnetic signatures of $\chi_{lf_{\min}}$ (B), χ_{fd} (C), χ_{arm} (D), SIRM and HIRM (E) parameters and χ_{arm}/SIRM ratio.

Table 10: The (un)mixing model source contribution estimates (%) to the Silolweni reservoir sediment.

Source	Summary values for the core				Downcore variability		
	Median	Percentile range (25% - 75%)	Uncertainty (75% - 25%)	Median goodness of fit (%) [range]	Sample median range	Sample percentile range (25% - 75%)	Median sample uncertainty [range]
Ecce Group	23	13 – 32	19	70 [3 - 90]	0 - 100	0 - 95	66 [6 - 100]
Granite	77	68 - 87			0 - 100	5 - 100	

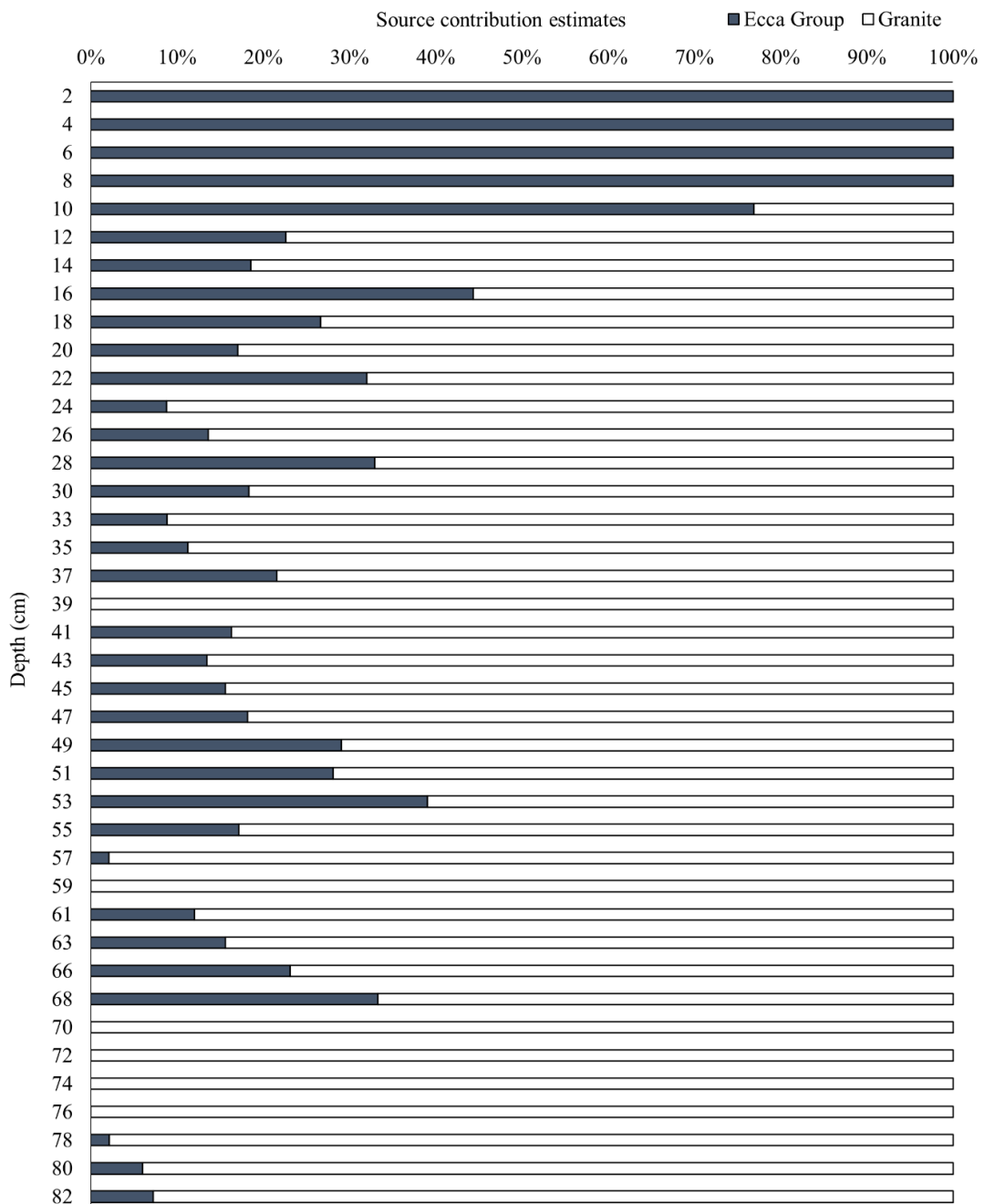


Figure 13: Median estimated contributions of the Silolweni sources.

5. DISCUSSION AND CONCLUSIONS

In a departure from normal practice, the <500 μm fraction was analysed because of the coarse nature of both the catchment and reservoir sediment. The <63 μm fraction made up a small proportion of all soils and sediments and most reservoir sediment samples fell within the 125 – 500 μm median particle size range. Peaks in down-core particle size were likely a result of coarser sediment transported during high energy storm events. In the Hartbeesfontein and Silolweni reservoir cores, changes in particle size were reflected in the mineral magnetic signatures. There was an increase in particle size and $\chi_{\text{lf}_{\text{min}}}$ and χ_{arm} signatures in the upper 10 cm of the Silolweni core (Figure 9), which corresponded to an increase in Eccla Group contribution estimates (Figure 10). In the Hartbeesfontein core, there was a coarsening of particle sizes when a decrease in mineral magnetic signatures was observed (Figure 4). Conservation of sediment properties between source and sink is an important assumption underlying sediment tracing. Potential dissolution was indicated in the lower sections Hartbeesfontein core. The values of $\chi_{\text{lf}_{\text{min}}}$ and χ_{arm} decreased markedly below 40 cm depth as this post-depositional process changes mineral magnetic assemblages by reducing the concentration of magnetic minerals (Anderson and Rippey, 1998). Statistical analyses of the full core and upper core section suggested the conservation of magnetic signatures could only be assumed in the upper core section. Tracer modelling was therefore restricted to this upper section. The presence of bacterial magnetite can also be indicative of post depositional changes. Although bacterial magnetite was indicated in all the reservoir sediments it was also found in the catchment soils so was not thought to be indicative of post-depositional changes in any of the reservoirs. No further confirmation tests for bacterial magnetite were undertaken as facilities were unavailable for further analysis.

Mineral magnetism effectively discriminated between signatures from distinctly different lithologies (e.g., between gabbro and granite gneiss in the Hartbeesfontein catchment and between sandstone and basalt in the Marheya catchment) and also between similar lithological formations (e.g., between gneiss and granite gneiss in the Hartbeesfontein catchment). These findings strengthen arguments made by D'Haen *et al.* (2012) and Laceby and Olley (2015), who show the efficacy of geology as a key discriminator for source modelling in areas minimally affected by human actions. In the semi-arid KNP environment where soil moisture becomes a key ecological driver, the underlying lithology has a direct impact on the overlying soil and vegetation cover. Granite, gneiss and rhyolite tend to produce coarse textured soils with a low water holding capacity and favour long rooted woody vegetation whereas basalt produces finer textured soils that support grassland. This

relationship between lithology, soil and vegetation increases the effectiveness of geology as a source provenance in this geographic location.

The ability of mineral magnetism to discriminate between lithologies allowed the application of an (un)mixing model to apportion sediment sources in each of the four catchments as highlighted in the contribution Walling and Oldfield (1979) made in their seminal paper suggesting that environmental magnetism could be used to help discriminate fluvial sediment sources. Over subsequent decades, environmental magnetism research has expanded and improved, and this research builds on the original contributions of authors like Walling to fluvial geomorphology.

The (un)mixing model estimated a total contribution from the granite gneiss lithology in the Hartbeesfontein catchment. The estimated sediment yield from this lithology ($204 \text{ t km}^{-2} \text{ yr}^{-1}$) was the highest calculated in this study. This estimated sediment yield was considerably higher than previous estimates for natural veld areas (Hoffman and Ashwell, 2001; Baade *et al.*, 2012). It is more similar to sediment yields from Australia and Europe. In small, gullied basins in the southern uplands of Australia, Wasson (1994) calculated sediment yields of $161 \pm 68 \text{ t km}^{-2} \text{ yr}^{-1}$ under native pasture lands. Vanmaercke *et al.* (2011) present a median sediment yield for Mediterranean catchments of $\sim 200 \text{ t km}^{-2} \text{ yr}^{-1}$. It is again noted that there were low sample numbers for this catchment. Although there is no direct erosion data for this lithology in KNP, this high yield suggests more factors were at play than just soil type. The potential drainage density was highest in this lithology (Table 1). Additionally, the wildlife tracks to the reservoir would have compacted soils, and there were large areas of exposed soil with no vegetation cover, increasing connectivity and erosion potential, supporting the findings of other erosion studies in South Africa by Meadows and Hoffman (2002), Poesen *et al.* (2003), Venter *et al.* (2003) Snyman and Du Preez (2005) Arthur *et al.* (2011). The reservoir was in the granite gneiss lithology so eroded sediment also had a short travel distance.

The sandstone lithology was estimated as the primary source of reservoir sediment in the Marheya catchment. The estimated sediment yield of the sandstone ($11 \text{ t km}^{-2} \text{ yr}^{-1}$) was double that of the basalt ($5 \text{ t km}^{-2} \text{ yr}^{-1}$). These estimated yields are within the natural-veld estimates of Hoffman and Ashwell (2001) ($2 - 75 \text{ t km}^{-2} \text{ yr}^{-1}$) and Baade *et al.* (2012) ($10 - 60 \text{ t km}^{-2} \text{ yr}^{-1}$), but below the estimates of Venter (1988) ($25 \text{ t km}^{-2} \text{ yr}^{-1}$). Droux *et al.* (2003) estimate a $20.5 \text{ t km}^{-2} \text{ yr}^{-1}$ sediment yield for a catchment on sandstone in Mali. The reservoir is in the sandstone lithology and this proximity, coupled with the shrubby vegetation, likely

increased the potential for sediment delivery compared to the grassier and more distant basalt source.

The weathering resistant rhyolite lithology was estimated as the primary source of reservoir sediment in the Nhlanganzwani catchment and had a higher sediment yield ($50 \text{ t km}^{-2} \text{ yr}^{-1}$) than the basalt lithology ($20 \text{ t km}^{-2} \text{ yr}^{-1}$). These estimated yields are within the range of estimates provided by Haylett (1960), Hoffman and Ashwell (2001) and Baade *et al.* (2012). The estimates are much lower than sediment yield estimates in Zimbabwean catchments with areas of 7 km^2 ($410 \text{ t km}^{-2} \text{ yr}^{-1}$), 7.1 km^2 ($157 \text{ t km}^{-2} \text{ yr}^{-1}$) and 8.6 km^2 ($469 \text{ t km}^{-2} \text{ yr}^{-1}$), respectively (Van den Wall Blake, 1986). Schmengler (2011) estimated sediment yields of 29.5 and $81.9 \text{ t km}^{-2} \text{ yr}^{-1}$ in two catchments in semi-arid southwestern Burkino Faso.

Rhyolite has a similar mineralogy to granite and the coarse textured soils support a sparse ground cover under woody bush. Furthermore, the steep rhyolite slopes and higher drainage density of the Lebombo Mountains would have favoured erosion, giving rise to increased sediment delivery and account for the higher contribution compared to the flatter basalt areas which also had a lower drainage density. This was the only catchment where relief was thought to be an important driver of sediment processes due to the generally low relief of the other catchments.

The (un)mixing model estimated the granite lithology as the primary source in the Silolweni catchment. This lithology also had a high sediment yield ($123 \text{ t km}^{-2} \text{ yr}^{-1}$) despite outcropping in the upper catchment at some distance from the reservoir. The sediment yield was higher than estimates by Haylett (1960), Hoffman and Ashwell (2001) and Baade *et al.* (2012) from similar lithology. The Eccca group lithology had a moderate sediment yield ($10 \text{ t km}^{-2} \text{ yr}^{-1}$). Soils were observed to be fine textured, with a good water holding capacity, but subject to capping when exposed. The gully system observed in the Eccca Group was near the reservoir and the increased contribution of this source to the upper reservoir core indicates that the gullying is recent.

The catchment sediment yields provided by Reinwarth *et al.* (2019) were refined in this study by attributing sediment yields to lithological sources. Reinwarth *et al.* (2019) extended their yield estimates to estimate erosion rates using a sediment delivery ratio based on catchment area, with the idea that sediment delivery ratio (SDR) decreases with increasing catchment size. Our research highlighted the fact that a partial area concept should be applied to sediment yield (Rowntree and Foster 2012), with some areas of a catchment contributing more sediment than others. Sediment yield, as recognised by Reinwarth *et al.* (2019), depends on both the in-situ erosion rate and the sediment delivery (connectivity). While

erosion is a function of lithology related factors such as soil type and vegetation, sediment delivery is a function not only of contributing area but also proximity to the sink and connectivity within the catchment, determined by drainage networks and slope gradient. The contributing area for sediment is also dynamic, depending on the interaction of runoff and temporal variations in vegetation cover. In the present study it was difficult to assign a sediment delivery ratio to individual lithologies, so no attempt was made to determine erosion rates.

The sediment source fingerprinting method using mineral magnetic tracers successfully discriminated between lithology catchment sources and estimated source contributions to reservoir sediment in a near-natural landscape. Sediment yields by lithology were calculated using source contribution estimates. Connectivity, travel distance, topography, and vegetation cover are key factors in influencing erosion potential of the catchments. The underlying lithology determines the magnetic signatures of the soils (discriminating sources), and the vegetation determines potential erosion rates, by acting as natural erosion mitigation measures in disrupting fluxes of water and sediment.

Lithology-based sources are recommended for future research in the KNP, with a minimum of 20 samples per source set. Analysing more than one reservoir core is also suggested. Potential future research from this study includes dating sediments and identifying flood events. A research focus could be placed on the affects of topography in sediment movement and yields. This study was the first mineral magnetic study in the KNP so the scope of future mineral magnetic research is wide. Following the research by Hanesch and Schloger (2015), potential changes in mineral magnetics with depth could be determined. Extensive sampling can compare similar lithology formations to understand spatial variability in mineral magnetic signatures (Pulley and Rowntree, 2016). If budget allows, additional tracers like geochemistry and fallout radionuclides could be used in the fingerprint. Bacterial magnetite presence could be confirmed using powder diffraction.

ACKNOWLEDGEMENTS

The authors thank SANParks Scientific Services in Skukuza for providing support during field campaigns under the research permit BAAJ1127. Financial support from the National Research Foundation (NRF, South Africa) and Deutsche Forschungsgemeinschaft (DFG, Germany Grant No: BA 1377/12-1) is acknowledged.

DATA AVAILABILITY

Data are available on request from the corresponding author.

REFERENCES

- Anderson, N. & Rippey, B., (1988). Diagenesis of magnetic minerals in the recent sediments of a eutrophic lake. *Limnology and Oceanography*, 33(2), 1476-1492.
- Anhaeusser, C.R. (2006). Ultramafic and mafic intrusions of the Kaapvaal Craton. In: Johnson, M.R., Anhaeusser, C.R. & Thomas, R.J. (eds) *The Geology of South Africa*. Geological Society of South Africa, Johannesburg/Council for Geoscience, Pretoria, 95–134.
- Arthur, E., Cornelis, W., Vermang, J. & De Rocker, E., (2011). Effect of compost on erodibility of loamy sand under simulated rainfall. *Catena*, 85(1), 67-72.
- Baade, J. & Schullius, C. (2015). Catchment properties in the Kruger National Park derived from the new TanDEM-X intermediate digital elevation model (IDEM). *Volume XL-7/W3, Proc. 36th International Symposium on Remote Sensing of Environment*, 11–15 May 2015, Berlin, Germany. 293-300.
- Baade, J., Franz, S. & Reichel, A. (2012). Reservoir siltation and sediment yield in the Kruger National Park, South Africa: a first assessment. *Land Degradation & Development*, 23(6), 586-600.
- Bartley, R., Roth, C., Ludwig, J., McJannet, D., Liedloff, A., Corfield, J., Hawdon, A. & Abbott, B. (2006). Runoff and erosion from Australia's tropical semi-arid rangelands: Influence of ground cover for differing space and time scales. *Hydrological Processes*, 20(15), 3317-3333.
- Blott, S. and Pye, K. (2001). GRADISTAT: A grain size distribution and statistics package for the analysis of unconsolidated sediments. *Earth Surface Processes and Landforms*, 26(11), 1237-1248.
- Brits, J., VanRooyen, M. & VanRooyen, N. (2002). Ecological impact of large herbivores on the woody vegetation at selected watering points on the eastern basaltic soils in the Kruger National Park. *African Journal of Ecology*, 40(1), 53-60.
- Boughey, A.S. (1957). The physiognomic delimitation of West African vegetation types. *Journal of the West African Science Association*, 3(2), pp.148-165.

- Cammeraat, E. (2004). Scale dependent thresholds in hydrological and erosion response of a semi-arid catchment in southeast Spain. *Agriculture, Ecosystems and Environment*, 104(2), 317-332.
- Collins, A.L. & Walling, D.E. (2007). Sources of fine sediment recovered from the channel bed of lowland groundwater-fed catchments in the UK. *Geomorphology*, 88(1-2), 120-138.
- Collins, A.L., Walling, D.E., & Leeks, G.J. (1997a). Source type ascription for fluvial suspended sediment based on a quantitative composite fingerprinting technique. *Catena*, 29, 1-27.
- Collins, A.L., Walling, D.E. & Leeks, G.J. (1997b). Use of the geochemical record preserved in floodplain deposits to reconstruct recent changes in river basin sediment sources. *Geomorphology*, 19(1-2), 151-167.
- Dearing, J.A. (1999). Holocene environmental change from magnetic proxies in lake sediments. In Maher, B. A., & Thompson, R. (eds) *Quaternary Climates, Environments and Magnetism*, Cambridge, Cambridge University Press, 231-278.
- Dearing, J.A. (2000). Natural magnetic tracers in fluvial geomorphology. In Foster, I.D.L. (ed) *Tracers in Geomorphology*. Chichester, John Wiley & Sons, 279-291.
- D'Haen, K., Verstraeten, G. & Degryse, P. (2012). Fingerprinting historical fluvial sediment fluxes. *Progress in Physical Geography*, 36(2), 154-186.
- Diop, S., Stapelberg, F., Tegegn, K., Ngubelanga, S. & Heath, L. (2011). A review on problem soils in South Africa. Council for Geoscience Report. Number: 2011-0062. Available at <https://www.geoscience.org.za/index.php/2017-05-24-21-07-23/problem-soils>
- Droux, J. P., Mietton, M., & Olivry, J. C. (2003). Flux de matières particulaires en suspension en zone de savane soudanienne: l'exemple de trois bassins versants maliens représentatifs/Suspended sediment yields in the Sudanian savanna zone: Examples from three representative catchments in Mali. *Géomorphologie: relief, processus, environnement*, 9(2), 99-110.
- Duncan, A. R. & Marsh, J. S. (2006). The Karoo Igneous Province. In Johnson, M. R., Anhaeusser, C. R., & Thomas, R. J. (eds) *The Geology of South Africa*, Pretoria, Geological Society of South Africa/Council for Geoscience, 501-520.

- Fatunbi, A. O., & Dube, S. (2008). Land degradation evaluation in a game reserve in Eastern Cape of South Africa: soil properties and vegetation cover. *Scientific Research and Essays*, 3(3), 111-119.
- Foster, I.D.L. & Boardman, J.B. (2018). The monitoring and assessment of land degradation: new approaches. In Boardman, J.B. & Holmes, P. (eds) *Land Degradation in Southern Africa*. London, Routledge, 249-274.
- Foster, I.D.L., Boardman, J.B. & Keay-Bright, J. (2007). Sediment tracing and environmental history for two small catchments, Karoo Uplands, South Africa. *Geomorphology*, 90(1-2), 126-143.
- Friedman, G.M. and Sanders, J.E. (1978). *Principles of Sedimentology*. Wiley.
- Garland, G.G., (1995). *Soil erosion in South Africa: A technical review*. Report for the Nat. Dept. Agric., Dir. Res. Cons. Dept. Geogr. and Env. Sci., Univ. Natal, Durban.
- Garland G.G., Hoffman T. & Todd S. (2000). Soil degradation. In Hoffman, T., Todd, S., Ntshona, Z., & Turner, S. (eds) *A national review of land degradation in South Africa*, Unpublished report, pp. 69–107. South African National Biodiversity Institute, Pretoria. Online at: <http://www.nbi.ac.za/landdeg>
- Gertenbach, W.D. (1980). Rainfall patterns in the Kruger National Park. *Koedoe*, 23(1), 35-43.
- Gertenbach, W.D. (1983). Landscapes of the Kruger National Park. *Koedoe*, 26(1), 9¹21.
- Grimshaw, H.M. (1989). Nutrient elements. In Allen, S.E. (ed) *Chemical Analysis of Ecological Materials*, Oxford, Blackwell, 81-159.
- Hatfield, R.G. & Maher, B.A. (2009). Fingerprinting upland sediment sources: Particle size-specific magnetic linkages between soils, lake sediments and suspended sediments. *Earth Surface Processes and Landforms*, 34(10), 1359-1373.
- Haylett, D.G. (1960). Run-off and soil erosion studies at Pretoria. *South African Journal of Agricultural Science* 3 (3), 379-394.
- Hoffman, T., & Ashwell, A. (2001). *Nature divided. Land degradation in South Africa*. University of Cape Town Press: Lansdowne, Cape Town, South Africa, 168 pp.
- Hooke, J. (2003). Coarse sediment connectivity in river channel systems: A conceptual framework and methodology. *Geomorphology*, 56(1-2), 79-94.

- Jacobs, S.M., Bechtold, J.S., Biggs, H.C., Grimm, N.B., Lorentz, S., McClain, M.E., Naiman, R.J., Perakis, S.S., Pinay, G. & Scholes, M.C. (2007). Nutrient vectors and riparian processing: A review with special reference to African semiarid savanna ecosystems. *Ecosystems*, 10(8), 1231-1249.
- Janssen, H. (2013). Monte-Carlo based uncertainty analysis: Sampling efficiency and sampling convergence. *Reliability Engineering and System Safety*, 109, 123-132.
- Johnson, M.R., VanVuuren, C.J., Visser, J.N., Cole, D.I., Wickens, H.D.V., Christie, A.D., Roberts, D.L. & Brandl, G. (2006). *Sedimentary rocks of the Karoo Supergroup*. In Johnson, M. R., Anhaeusser, C. R., & Thomas, R. J. (eds) *The Geology of South Africa*, Pretoria, Geological Society of South Africa/Council for Geoscience, 461-499.
- Kakembo, V., Ndlela, S. & Cammeraat, E. (2012). Trends in vegetation patchiness loss and implications for landscape function: The case of *Pteronia Incana* invasion in the Eastern Cape Province, South Africa. *Land Degradation and Development*, 23(6), 548-556.
- Kotzé, E., Sandhage-Hofmann, A., Meinel, J.A., Du Preez, C.C. & Amelung, W. (2013). Rangeland management impacts on the properties of clayey soils along grazing gradients in the semi-arid grassland biome of South Africa. *Journal of Arid Environments*, 97, 220-229.
- Kraushaar, S., Schumann, T., Ollesch, G., Schubert, M., Vogel, H.J. & Siebert, C. (2015). Sediment fingerprinting in northern Jordan: Element-specific correction factors in a carbonatic setting. *Journal of Soils and Sediments*, 15(10), 2155-2173.
- Lacey, J.P. & Olley, J.M. (2015). An examination of geochemical modelling approaches to tracing sediment sources incorporating distribution mixing and elemental correlations. *Hydrological Processes*, 29(6), 1669-1685.
- Laker, M.C. (2004). Advances in soil erosion, soil conservation, land suitability evaluation and land use planning research in South Africa, 1978–2003. *South African Journal of Plant and Soil*, 21(5), 345-368.
- Lange, R.T. (1969). The piosphere: Sheep track and dung patterns. *Rangeland Ecology and Management/Journal of Range Management Archives*, 22(6), 396-400.
- Le Roux, J.J., Morgenthal, T.L., Malherbe, J., Pretorius, D.J. & Sumner, P.D. (2008). Water erosion prediction at a national scale for South Africa. *Water SA*, 34(3), 305-314.

- Lees, J.A. (1997). Mineral magnetic properties of mixtures of environmental and synthetic materials: Linear additivity and interaction effects. *Geophysical Journal International*, 131(2), 335-346.
- Maher, B.A. (1986). Characterisation of soils by mineral magnetic measurements. *Physics of the Earth and Planetary Interiors*, 42(1-2), 76-92.
- Maher, B.A. (1998). Magnetic properties of modern soils and Quaternary loessic paleosols: Paleoclimatic implications. *Palaeogeography, Palaeoclimatology, Palaeoecology*, 137(1-2), 25-54.
- Manjoro, M. (2011). *Soil erosion and sediment source dynamics of a catchment in the Eastern Cape Province, South Africa: An approach using remote sensing and sediment source fingerprinting techniques*. Unpublished PhD Thesis, Nelson Mandela Metropolitan University, Port Elizabeth.
- Manjoro, M., Rowntree, K.M., Kakembo, V. & Foster, I.D.L. (2012). Gully fan morphodynamics in a small catchment in the Eastern Cape, South Africa. *Land Degradation and Development*, 23(6), 569-576.
- Mati, B.M. & Veihe, A. (2001). Application of the USLE in a savannah environment: Comparative experiences from East and West Africa. *Singapore Journal of Tropical Geography*, 22(2), 138-155.
- McKinley, R., Radcliffe, D. & Mukundan, R. (2013). A streamlined approach for sediment source fingerprinting in a Southern Piedmont watershed, USA. *Journal of Soils and Sediments*, 13(10), 1754-1769.
- Meadows, M.E. & Hoffman, M.T. (2002). The nature, extent and causes of land degradation in South Africa: Legacy of the past, lessons for the future? *Area*, 34(4), 428-437.
- Molles, M. & Cahill, J.F. (1999). *Ecology: Concepts and Applications*. Boston, McGraw-Hill Education.
- Mucina, L. & Rutherford, M.C. (2006). *The vegetation of South Africa, Lesotho and Swaziland*. Pretoria, South African National Biodiversity Institute.
- Munyati, C. & Ratshibvumo, T. (2010). Differentiating geological fertility derived vegetation zones in Kruger National Park, South Africa, using Landsat and MODIS imagery. *Journal for Nature Conservation*, 18(3), 169-179.

- Mzuza, M. K., Zhang, W., Kapute, F., & Selemani, J. R. (2017). Magnetic properties of sediments from the Pangani River Basin, Tanzania: Influence of lithology and particle size. *Journal of Applied Geophysics*, *143*, 42-49.
- Nangula, S. & Oba, G. (2004). Effects of artificial water points on the Oshana ecosystem in Namibia. *Environmental Conservation*, *31*(1), 47-54.
- Olley, J.M. & Caitcheon, G.G. (2000). Major element chemistry of sediments from the Darling–Barwon river and its tributaries: Implications for sediment and phosphorus sources. *Hydrological Processes*, *14*(7), pp.1159-1175.
- Pienaar, U.D. (1985). Indications of progressive desiccation of the Transvaal Lowveld over the past 100 years, and implications for the water stabilization programme in the Kruger National Park. *Koedoe*, *28*(1), 93-165.
- Poesen, J., Nachtergaele, J., Verstraeten, G. & Valentin, C. (2003). Gully erosion and environmental change: Importance and research needs. *Catena*, *50*(2-4), 91-133.
- Pulley, S. (2014). *Exploring fine sediment dynamics and the uncertainties associated with sediment fingerprinting in the Nene river basin, UK*. Unpublished PhD Thesis, University of Northampton, UK.
- Pulley, S. & Rowntree, K.M. (2016). Stages in the life of a magnetic grain: Sediment source discrimination, particle size effects and spatial variability in the South African Karoo. *Geoderma*, *271*, 134-143.
- Pulley, S., Foster, I.D. & Antunes, P. (2015a). The uncertainties associated with sediment fingerprinting suspended and recently deposited fluvial sediment in the Nene river basin. *Geomorphology*, *228*, 303-319.
- Pulley, S., Rowntree, K.M. & Foster, I.D.L. (2015b). Conservatism of mineral magnetic signatures in farm dam sediments in the South African Karoo: The potential effects of particle size and post-depositional diagenesis. *Journal of Soils and Sediments*, *15*(12), pp.2387-2397.
- Reid, K.D., Wilcox, B.P., Breshears, D.D. & MacDonald, L. (1999). Runoff and erosion in a Piñon–Juniper woodland influence of vegetation patches. *Soil Science Society of America Journal*, *63*(6), 1869-1879.
- Reinwarth, B., Miller, J.K., Glotzbach, C., Rowntree, K.M. and Baade, J., 2017. Applying regularized logistic regression (RLR) for the discrimination of sediment facies in

- reservoirs based on composite fingerprints. *Journal of Soils and Sediments*, 17(6), pp.1777-1795.
- Reinwarth, B., Riddell, E.S., Glotzbach, C., Baade, J. (2018). Estimating the sediment trap efficiency of intermittently dry reservoirs: lessons from the Kruger National Park, South Africa. *Earth Surface Processes* 43 (2), 463–481.
<https://doi.org/10.1002/esp.4263>.
- Reinwarth, B., Petersen, R. & Baade, J. (2019). Inferring mean rates of sediment yield and catchment erosion from reservoir siltation in the Kruger National Park, South Africa: An uncertainty assessment. *Geomorphology*, 324(1), 1-13.
- Rowntree, K.M. & Foster I.D.L. (2012). A reconstruction of historical changes in sediment sources, sediment transfer and sediment yield in a small, semi-arid Karoo catchment, South Africa. *Zeitschrift fur Geomorphology*. 56, Suppl. Bd. 1, 87-98.
- Rowntree, K. M., van der Waal, B. W., & Pulley, S. (2017). Magnetic susceptibility as a simple tracer for fluvial sediment source ascription during storm events. *Journal of environmental management*, 194, 54-62.
- SANParks (South African National Parks). (2008). *Media release: Dam drained in KNP to prevent animal deaths*. SANParks: Skukuza.
- Schmengler, A. C. (2011). *Modeling soil erosion and reservoir sedimentation at hillslope and catchment scale in semi-arid Burkina Faso* (Doctoral dissertation, Universitäts-und Landesbibliothek Bonn).
- Snyman, H.A. & Van Rensburg, W.L. (1986). Effect of slope and plant cover on run-off, soil loss and water use efficiency of natural veld. *Journal of the Grassland Society of Southern Africa*, 3(4), 153-158.
- Snyman, H.D. & Du Preez, C.C. (2005). Rangeland degradation in a semi-arid South Africa - II: Influence on soil quality. *Journal of Arid Environments*, 60(3), 483-507.
- Stewart, D.A. & Samways, M.J. (1998). Conserving dragonfly (Odonata) assemblages relative to river dynamics in an African savanna game reserve. *Conservation Biology*, 12(3), 683-692.
- Toy, T.J., Foster, G.R. & Renard, K.G. (2002). *Soil erosion: Processes, prediction, measurement, and control*. Chichester, Wiley.

- Van den Wall Bake, G. W. (1986). Siltation and soil erosion survey in Zimbabwe. *IAHS-AISH publication*, (159), 69-80.
- van der Waal, B.W. (2014). *Sediment connectivity in the upper Thina Catchment, Eastern Cape, South Africa*. Unpublished PhD Thesis, Rhodes University, South Africa.
- van der Waal, B.W., Rowntree, K.M. & Pulley, S. (2015). Flood bench chronology and sediment source tracing in the upper Thina catchment, South Africa: The role of transformed landscape connectivity. *Journal of Soils and Sediments*, 15(12), 2398-2411.
- Vanmaercke, M., Poesen, J., Broeckx, J. & Nyssen, J. (2014). Sediment yield in Africa. *Earth-Science Reviews*, 136, 350-368.
- Venter, F.J. (1986). Soil patterns associated with the major geological units of the Kruger National Park. *Koedoe*, 29(1), 125-138.
- Venter, F.J. (1988). *Soil loss and run-off in Umfolozi Game Reserve and the implications for game reserve management*. Volume 1. Unpublished PhD Thesis. Department of Grassland Science, Faculty of Agriculture, University of Natal: Pietermaritzburg, South Africa.
- Venter, F.J. & Bristow, J.W. (1986). An account of the geomorphology and drainage of the Kruger National Park. *Koedoe*, 29(1), 117-124.
- Venter, F.J. & Gertenbach, W.D. (1986). A cursory review of the climate and vegetation of the Kruger National Park. *Koedoe*, 29(1), 139-148.
- Venter, F.J., Scholes, R.J. & Eckhardt, H.C. (2003). *The abiotic template and its associated vegetation pattern*. In DuToit, J.T., Rogers, K.H. & Biggs, H.C. (eds) *The Kruger Experience: Ecology and Management of Savanna Heterogeneity*, Washington, Island Press, 83-129.
- Walden, J. (1999). *Sample collection and preparation*. In Walden, J., Oldfield, F. & Smith, J. (eds) *Environmental Magnetism: A Practical Guide. Technical Guide*, (6), London, Quaternary Research Association, 26-34.
- Walden, J., Slattery, M. C., & Burt, T. P. (1997). Use of mineral magnetic measurements to fingerprint suspended sediment sources: approaches and techniques for data analysis. *Journal of Hydrology*, 202(1-4), 353-372.

- Walling, D.E. & Oldfield, F. (1979). Suspended sediment sources identified by magnetic measurements. *Nature*, 281, 110-113.
- Walling, D.E. & Webb, B.W. (1996). Erosion and sediment yield: A global overview. *IAHS Publication*, 236, 3-20.
- Wessels, K.J. & Dwyer, P.C. (2011). *Impact of ENSO events on the Kruger National Park's vegetation*. Stellenbosch, Sun Media.
- White, P.S. (1979). Pattern, process, and natural disturbance in vegetation. *The Botanical Review*, 45(3), 229-299.
- Wilcox, B.P., Davenport, D.W., Pitlick, J. & Allen, C.D. (1996). Runoff and erosion from a rapidly eroding pinyon-juniper hillslope. *Journal of Range Management*, 47, 285-295.
- Wilkinson, S.N., Hancock, G.J., Bartley, R., Hawdon, A.A. & Keen, R.J. (2013). Using sediment tracing to assess processes and spatial patterns of erosion in grazed rangelands, Burdekin River basin, Australia. *Agriculture, Ecosystems and Environment*, 180, 90-102.
- Zhang, W., Xing, Y., Yu, L., Feng, H., & Lu, M. (2008). Distinguishing sediments from the Yangtze and Yellow Rivers, China: a mineral magnetic approach. *The Holocene*, 18(7), 1139-1145.